The University of Alberta
Printing Department
Edmonton, Alberta

THE UNIVERSITY OF ALBERTA

THE EFFECT OF TEMPERATURE ON ION COLLECTION IN GAS PHASE RADIOLYSIS CELLS

BY

R. M. BYRTUS 

A THESIS

SUBMITTED TO THE FACULTY OF GRADUATE STUDIES

IN PARTIAL FULFILMENT OF THE REQUIREMENTS FOR THE DEGREE

OF MASTER OF SCIENCE

DEPARTMENT OF CHEMISTRY

EDMONTON, ALBERTA

JULY, 1968

UNIVERSITY OF ALBERTA

FACULTY OF GRADUATE STUDIES

The undersigned certify that they have read, and recommend to the Faculty of Graduate Studies for acceptance, a thesis entitled "The Effect of Temperature on Ion Collection in Gas Phase Radiolysis Cells" submitted by R. M. Byrtus in partial fulfilment of the requirements for the degree of Master of Science in Chemistry.

A B S T R A C T

The effect of temperature on ion collection in gas phase radiolysis cells was investigated. In Pyrex radiolysis cells the saturation current is lowered by temperature increases above 50°C up to approximately 120°C where good plateaus start to disappear.

A study of the conductance of a Pyrex plug indicated that that the conductance of Pyrex complicates the saturation current measurements at the elevated temperatures. When the conductance of Pyrex becomes appreciable at temperatures greater than 50°C, the Pyrex cell wall acts as a collecting electrode. Some of the gaseous ions are collected by the Pyrex wall and conducted to ground by the ionized air. At temperatures greater than 120°C, the ionized gas current is concealed by the large current due to the conductance of Pyrex.

When the outer surface of the Pyrex cell is insulated from the ionized air, all of the gaseous ions are collected by the metal electrodes and the saturation current is essentially independent of temperature. When the outer surface of the Pyrex cell is painted with aquadag and grounded with a copper wire, the grounding of the Pyrex wall is improved, and a greater number of the gaseous ions are diverted from the metal electrodes.

Temperature independent currents were obtained in a parallel-plate Quartz cell and in a well insulated stainless steel spherical cell. Quartz does not conduct appreciably when heated to 170°, and the insulation of the stainless steel prevents any current from being collected by or from the ionized air. Consequently true saturation currents are measured.

ACKNOWLEDGEMENTS

The author would like to thank Prof. G. R. Freeman for his guidance and patience during the course of this project.

Thanks are also extended to the members of the radiation chemistry group and the technical staff for their assistance.

TABLE OF CONTENTS

	Page
Abstract	iii
Acknowledgements	v
Table of Contents	vi
List of Tables	xi
List of Figures	xii
1. Introduction	1-17
1. Radiation Chemistry	
A. Definition	1
B. History	1
2. Radiation Source	3
3. Interaction of Electromagnetic Radiation with Matter	
A. Attenuation of X- and γ-rays	3
B. Photoelectric Effect	5
C. Compton Effect	5
D. Pair Production	6
4. Energy Transfer from Compton Electrons	7
A. Energy Loss by Inelastic Collisions	7
B. Energy Loss by Radiation	9
C. Elastic Scattering of Electrons	10
5. Dosimetry	
A. Definition	10
a. Roentgen	11
b. Rad	11

B. Calorimetry 11

C. Actinometry 11

D. Ionization Methods 12

a. α-particles 12

b. X- and γ-rays 13

i. Standard Air Chamber 13

ii. "Air-wall" Chambers 14

iii. Radiolysis Cells 16

6. Observed Temperature Effect on Ion Collection in Radiolysis Cells 16

II. Experimental 18-29

1. Gases Used for Radiolysis 18

2. Radiolysis Cells 18

A. Pyrex Parallel-plate Cell 18

B. Parallel-plate Cell with Guard Ring 20

C. Parallel-plate Cell with a Kovar Section in the Stem of the Cell 20

D. Parallel-plate Cell with Aluminium Electrodes that Did Not Touch the Walls 21

E. Pyrex Spherical Cell 21

F. Conducting Plugs 21

G. Ceramic Cell 21

H. Stainless-steel Spherical Cell 24

3. Preparation of Samples

A. Preparation of Cells 24

B. Filling of the Cells 25

4. Irradiation of the Samples 25

5. Electrical Circuit and Current Measurement 27

III. Results 30-65

1. Pyrex Radiolysis Cells

A. Temperature Effect in Different Gases, Parallel-plate Electrodes 30

B. Different Electrode Materials in Parallel-plate Cells 36

C. Effect of Guard Rings in Parallel-plate Cells 38

D. Effect of Conditioning the Cell 42

E. Cleaning and Grounding the Outer Surface of the Cell 42

F. Variation of d/l for Cell with Parallel-plate Aluminium Electrodes 44

G. Pyrex Spherical Cell 47

H. Conductance of a Pyrex Plug 47

I. Effect of Wrapping Outer Surface of Cell and of Plug with Teflon Tape 53

2. Conductance of Ceramic 55

3. Quartz Cell

A. Conductance of Quartz 56

B. Temperature Effect in a Quartz Cell with Parallel-plate Electrodes 56

4. Steel Spherical Cell 58

5. Dose Rate Effect 58

IV. Discussion 66-89

1. Effects Observed in Pyrex Cells with Metal Electrodes 66

2. Reasons Why These Effects Were Unexpected

A. Temperature Coefficient of Ionization is Negligible 67

B. Recombination Coefficients Decrease as the Temperature Increases 69

C. Space Charges at the Electrodes Should Not Affect the Saturation Currents 73

D. Effect Too Large for Ion Loss by Diffusion to the Walls 75

E. Photoelectric Effect Should Have No Effect on the Number of Electrons Released as the Temperature is Varied Over the Range Used 79

3. Interpretation of Effects in Pyrex Cell

A. General Interpretation of Effects 79

B. Pyrex Plug 82

C. Parallel-plate Cell 83

D. Spherical Cell 87

4. Temperature Independent Currents Were Obtained in Quartz Cell 87

5. Dose Rate Studies 88

6. Temperature Independent Currents in Externally Insulated Spherical Stainless Steel Cell 89

References 90-91

LIST OF TABLES

Table		Page
III-1	Temperature Effect on Saturation Currents	31
III-2	Effect of Different Electrode Materials on Saturation Currents	39
III-3	Conductance of a Pyrex Plug	51
III-4	Conductance of a Pyrex Plug Wrapped With Teflon Tape	52
III-4a	Conductance of a Supramica 500 Plug	55
III-5	Conductance of a Quartz Plug	57
III-6	Dose Rate Effect on Net Saturation Current	62

LIST OF FIGURES

Figure		Page
I-1	Mass Absorption Coefficients for Air as a Function of Photon Energy	8
I-2	Dependence of the Current Density on the Electric Field	14
II-1	Cells for Measurements of Saturation Currents	19
II-2	Spherical Cell and Conducting Plug	22
II-3	Radiolysis Cells	23
II-4	Gas Storage and Radiolysis Filling System	26
II-5	Electrical Circuit	28
III-1	Currents Measured in Pyrex Cell with Aluminium Electrodes (air)	32
III-2	Currents Measured in Pyrex Cell with Aluminium Electrodes (argon)	33
III-3	Currents Measured in Pyrex Cell with Aluminium Electrodes (helium)	34
III-4	Currents Measured in Pyrex Cell with Aluminium Electrodes (hydrogen)	35
III-5	Currents Measured in Pyrex Cell with Aluminium Electrodes (helium and air at 25° and -196°C)	37
III-6	Circuit for Parallel-plate Cell with Guard Ring	41
III-7	Currents Measured in Pyrex Cell with Aluminium Electrodes (Net Currents in Conditioned Cell and Net Current when Different Surface Areas were Grounded)	45

Figure		Page
III-8	Decrease in Saturation Currents with Temperature at Different Pressures When Side of Pyrex Cell with Aluminium Electrodes Painted with Aquadag and Grounded	46
III-9	Percent Decrease in Saturation Current for Different Ratios of Diameter (d) of Electrodes to Distance (l) Between Electrodes	48
III-10	Currents Measured in Pyrex Spherical Cell (air)	49
III-11	Currents Measured in Pyrex Spherical Cell (helium)	50
III-12	Currents Measured in Pyrex Spherical Cell Wrapped with Teflon Tape	54
III-13	Saturation Currents in Stainless Steel Spherical Cell (hydrogen)	59
III-14	Dose Rate Effect in Pyrex Cell with Aluminium Electrodes (hydrogen)	63
III-15	Dose Rate Effect (air)	64
III-16	Dose Rate Effect in Quartz Cell with Stainless Steel Electrodes (hydrogen)	65
IV-1	Interpretation of Effects in Pyrex Cells	87

I N T R O D U C T I O N

1. RADIATION CHEMISTRY

A. Definition (1)

Radiation Chemistry is the study of chemical changes that are induced by high energy radiation.

The high energy radiations with which radiation chemistry is concerned include the chemical effects produced by radiation from radioactive nuclei (α-, β-, and γ-rays), by high energy charged particles (electrons, protons, deuterons, and He ions), and by X-rays. Since high energy radiation causes ionization of the medium in which it is absorbed, it is sometimes called "ionizing radiation".

B. History (2)

Radiation Chemistry can be said to have its origin with the discovery of X-rays by Roentgen in 1895, radioactivity of uranium by Becquerel in 1896, radium and polonium by the Curies in 1898. The observation of some of the remarkable effects of the radiation from radium followed soon after its discovery.

The early studies of the effects of radiation on gases were mainly carried out by S.C. Lind and co-workers in the United States and by W. Mund and associates in Belgium. These studies were mainly carried out by exposing the gases to the α-particles of radium or radon. Lind attempted to

determine the relationship between the number of ion pairs formed by α-rays in a gas and the number of molecules undergoing chemical change. In many systems he found that the ionic yield, M/N, defined as the number of molecules formed or destroyed per ion pair, exceeded unity. This was attributed to reaction of ions with neutral molecules to form clusters about the central ion which could lead to reaction products (via excited molecules) upon neutralization of the ion.

The ion-cluster theory could explain some experimental observations, but later work raised objection to the adoption of the theory as a general mechanism for radiation-chemical reactions and to the supposition that ions are the sole precursors of chemical effects. Firstly, Eyring, Hirschfelder, and Taylor calculated that large clusters were theoretically improbable and also pointed out that the average energy lost in forming an ion pair in a gas (W) is appreciably greater than the first ionization potential (I) for the gas. It was concluded that the excess energy (W - I) could be used to form electronically excited molecules. Both ions and excited molecules could give rise to free radicals. Secondly, Essex and his co-workers, studied gaseous reactions induced by α-particles both in the presence and absence of an electric field. It was found that even in the presence of the field, when ion neutralization in the gas phase should be eliminated or much reduced, the chemical yield is not greatly affected.

It is now accepted that both ions and excited

molecules are formed initially during the absorption of the ionizing radiation and that free radicals are generally produced and play an important part in the chemical reactions which follow.

2. RADIATION SOURCE (2)

Gamma radiation from a cobalt-60 source was used for the experimental work done in this project. Cobalt-60 is a radioactive isotope prepared from naturally occuring cobalt-59 by irradiating it in a nuclear reactor. During the formation of cobalt-60 a neutron is absorbed and a γ-ray is emitted. The cobalt-60 nucleus decays with the emission of a β-particle (fast electron) and gamma rays (1.17 and 1.33 MeV), forming stable nickel-60.

The activity (C_t) of a source after a period of decay (t) is related to the original activity (C_o) by the expression

$$(C_t)/(C_o) = e^{-\lambda t} \text{ ----------(I-1)}$$

where λ is the decay constant (λ = 0.693/half-life). Thus the activity of a cobalt-60 source, which has a half-life of 5.27 years falls by 1.1% per month.

3. INTERACTION OF ELECTROMAGNETIC RADIATION WITH MATTER (1)

A. Attenuation of X- and γ-rays

For high energy radiation to cause chemical reactions in matter energy must be transferred from the radiation to the

matter. When photons (X-or γ-rays) pass through matter, the number of photons transmitted through a slice of absorber of thickness dx decreases exponentially on traversing an increasing thickness of an absorbing medium, according to the equation

$$I = I_o e^{-\mu x} \text{ ----------(I-2)}$$

where I_o = intensity of beam incident upon absorber

I = intensity of beam after passage through thickness X of absorber

μ = linear absorption coefficient

The linear absorption coefficient corresponds to the sum of several processes which contribute to the absorption of energy from photons by matter.

(a) photoelectric effect - important mostly at photon energies < 0.1 MeV.

(b) Compton effect - important for energies $\doteq$ 0.01 - 100 MeV.

(c) pair production - important for energies > 5 MeV.

(d) photo-disintegration of the nucleus - often important at energies > 10 MeV.

Processes (a), (b) and (c) account for the attenuation of X- and γ-rays over the energy range usually encountered in radiolytic studies. Thus the linear absorption coefficient may be expressed as

$$\mu = \tau + \sigma + \pi \text{ ----------(I-3)}$$

where τ = photoelectric absorption coefficient

σ = Compton absorption coefficient

π = pair production absorption coefficient

B. Photoelectric Effect

In this process the photon gives up all its energy to an extranuclear electron, and the electron is ejected from the atom or molecule with all the energy of the incident photon minus the original binding energy of the electron,

$$T = h\nu - w \qquad \text{(I-4)}$$

where T = kinetic energy of ejected electron

w = binding energy of ejected electron when in the atom

As the absorption coefficient per electron is dependent upon the average binding energy, it is a function of the effective atomic number of the medium. It has been experimentally observed that the atomic photoelectric absorption coefficient is approximately proportional to the fourth power of atomic number.

The photoelectric effect is of greatest importance for radiation of low energy and for material of high atomic number.

C. Compton Effect

In the Compton effect a photon "collides" with either a bound or free electron. The electron is accelerated and the photon is scattered with reduced energy.

$$T = h(\Delta\nu) - w \qquad \text{(I-5)}$$

where T = kinetic energy of the electron

$\Delta\nu$ = change in frequency of the photon

w = original binding energy of the electron

The atomic Compton absorption coefficient is independent of the field of the nucleus and therefore depends only on the number of electrons in the atom.

The amount of energy absorbed by a system will be the initial energy of the photon minus the energy of the scattered photon. The total Compton coefficient may be expressed as the sum of two partial coefficients:

$$\sigma t = \sigma a + \sigma s \text{ ----------(I-6)}$$

where σt = total Compton coefficient

σa = true or actual Compton absorption coefficient

σs = Compton scatter coefficient

The value of σa and σs depend upon the energy of the photon. For photons with energies in the vicinity of 1 MeV (Co^{60} region), $\sigma a \doteq \sigma s$.

D. Pair Production

Pair production involves the complete absorption of a photon, resulting in the production of an electron - positron pair. The kinetic energy of the electron and positron is the energy of the photon less the rest mass energies of the two particles ($E = 2m_o c^2 = 1.02$ MeV) and the nuclear recoil energy, i.e.,

$$T(e^+ = e^-) = h\nu - 1.02 \text{ MeV} - \text{nuclear recoil energy (small)} \text{ ----------(I-7)}$$

Because the total rest mass energy is 1.02 MeV the energy of the photon must be greater than 1.02 MeV.

When the positron is slowed down to thermal energy, it annihilates with an electron, and the two particles are replaced by two 0.51 MeV gamma rays.

The pair production absorption coefficient is proportional to the square of the atomic number of the absorber and increases with increasing photon energy.

The important absorption process occuring when Co^{60} γ-rays interact with substances of low atomic number is the Compton process. The relative importance of the three main energy absorption processes occuring in air at various photon energies is illustrated in Fig. I - 1.

4. ENERGY TRANSFER FROM COMPTON ELECTRONS (1)

Compton electrons interact with matter principally by inelastic and elastic collisions and by the emission of electromagnetic radiation. The importance of these processes depends upon the energy of the incident electrons and upon the nature of the absorbing material.

A. Energy Loss by Inelastic Collisions

When the velocity of the incident electron exceeds that of the atomic orbital electrons, the electron transfers energy to the electrons of the atom, producing excited and ionized atoms or molecules. Bethe derived an equation for the rate of energy loss of a high energy electron per unit path length in a medium:

FIGURE I - 1

Mass Absorption Coefficients for Air as a Function of Photon Energy

The density of air (ρ) is 0.001293 gm/cm^3 at STP.

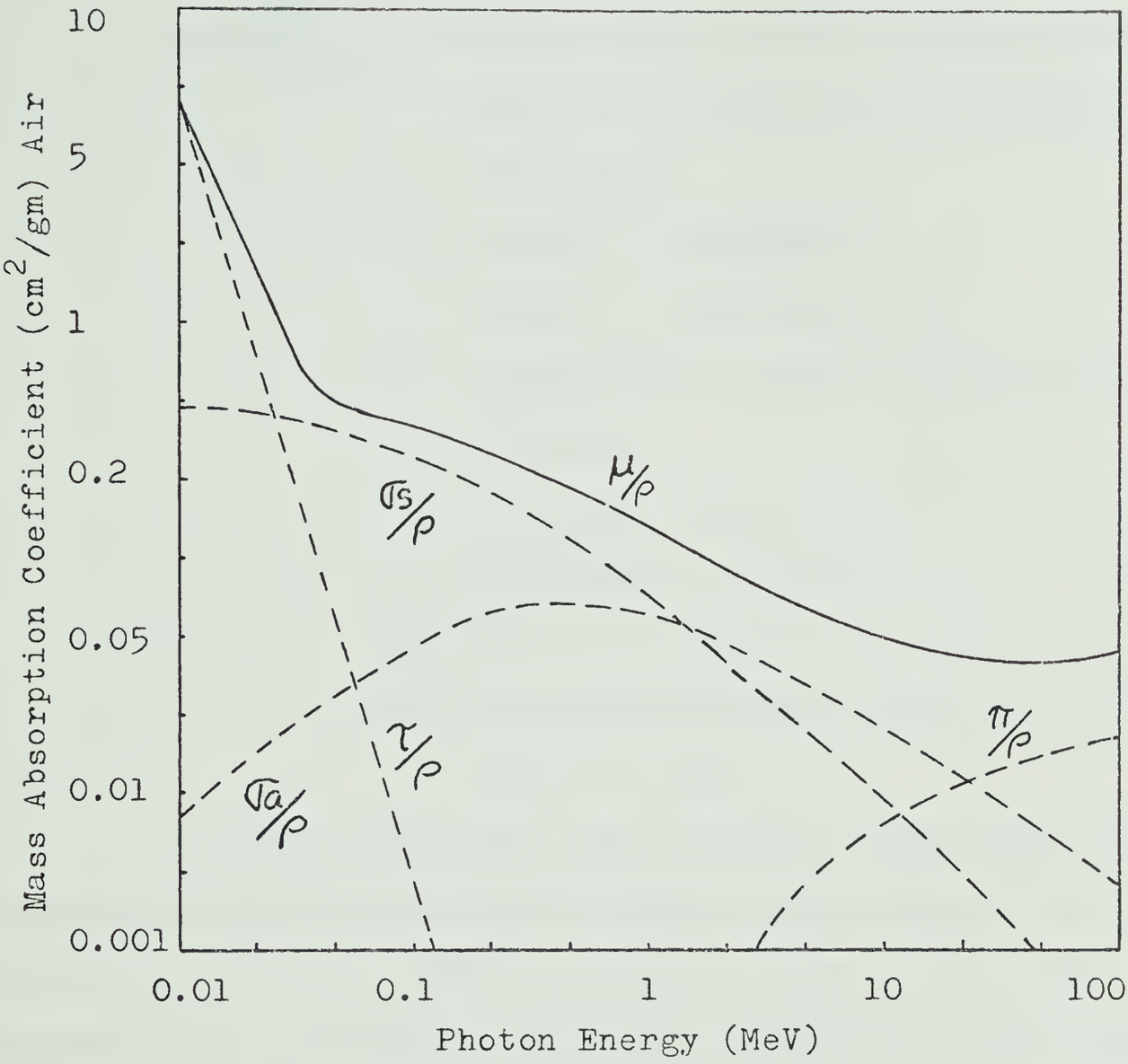
Mass Absorption Coefficient (cm²/gm) Air
10
5
1
0.2
0.05
0.01
0.001
0.01
0.1
1
10
100
Photon Energy (MeV)
μ/ρ
σs/ρ
σa/ρ
τ/ρ
π/ρ

$$-\left(\frac{dt}{dx}\right)_{coll} = \frac{2\pi e^4 ZN}{m_o v^2}\left[\ln \frac{m_o v^2 T}{2I^2(1-\beta^2)} - \left(2\sqrt{1-\beta^2} - 1 + \beta^2\right)\ln Z + (1-\beta^2) + 1/8\left(1-\sqrt{1-\beta^2}\right)^2\right]$$

where $\left(\frac{dt}{dx}\right)_{coll}$ = collisional loss of kinetic energy in ergs per increment of path length, dx, in cm

N = number of atoms/cm^3

Z = number of electrons/atom

T = relativistic kinetic energy of the electron

m_o = rest mass of an electron

v = velocity of the electron

β = v/c, c = velocity of light

I = average excitation potential of the atom, in ergs

It can be noted that the specific energy loss is proportional to the electron density of the medium, is a minimum for an electron with an energy of about 1 MeV, and decreases with increasing excitation potential of the matter through which the electron is passing.

B. Energy Loss by Radiation

When fast electrons pass close to the nucleus of an atom they may be rapidly decelerated and the energy is lost in the form of photon emission. The rate of energy loss is pro-

portional to the relativistic energy of the electron and to the square of the atomic number of the stopping medium. This process commences at electron energies of about 1 MeV and increases in importance with increasing energy.

The approximate relative magnitudes of the collisional and radiative energy losses are indicated by the expression

$$\frac{(dt/dx)_{coll}}{(dt/dx)_{rad}} = \frac{1600\ m_o c^2}{TZ}$$

C. Elastic Scattering of Electrons

When a collision is elastic, the electron is scattered without loss of energy. Electrons have a small mass and are very easily deflected by the Coulomb fields of the nuclei and bound electrons in the medium. Elastic scattering is greatest for low energy electrons and for high atomic number materials.

The intensity of a narrow beam of electrons might be greatly decreased by elastic scattering of electrons out of the beam.

5. DOSIMETRY (1)

A. Definition

Dosimetry involves the measurement of the amount of energy absorbed by the irradiated system. The two commonly used dose units are the roentgen and the rad.

(a) Roentgen

A roentgen is the quantity of X- or γ-radiation required to produce one e.s.u. (2.083×10^9 electron charges) of charge of either sign in 1 cm^3 of dry air at STP (1.293 mg dry air). Thus, the roentgen measures a certain effect in air and is not a direct measure of energy absorbed in any given medium. Since the energy required to form an ion pair in air is 34 eV, the roentgen corresponds to an energy absorption of 88 ergs per gram of dry air.

(b) Rad

A rad is the absorption of 100 ergs (6.24×10^{13} eV) per gram of absorber. Due to the uncertainty in calculating absorbed dose in a condensed system from the number of ion pairs produced in air, the rad is a more appropriate unit for liquids and solids than is the roentgen.

B. Calorimetry

Calorimetry can be used to measure the energy absorbed by an irradiated system in the form of heat if no chemical changes occur in the medium that is irradiated. This method of dosimetry cannot be used for gases because of their low density.

C. Actinometry (Chemical Dosimetery)

Energy absorbed in a homogeneous or non-homogeneous

radiation field can be calculated by measuring the amount of chemical change per unit time that is produced in a system whose behavior is known.

The chemical yield in a good actinometer should be independent of:

(i) dose rate and total dose

(ii) moderate changes in pH, temperature, concentration of reactant, etc.

(iii) traces of impurities

(iv) nature and energy of radiation.

In addition, the measurement should be rapid and easy, no pre- or post- irradiation reaction should occur in the system, and the absorption properties of the actinometer should be nearly the same as that of the sample.

The actinometer which most nearly satisfies these requirements over the total dose region 1 to 50 kilorads is the Fricke dosimeter (1 mM Fe^{2+} and 1 mM Cl^- in 0.8 N H_2SO_4).

D. Ionization Methods

Ionization methods usually involve the measurement of ionization in air. Any other gas whose W value is well established can be used, but air is the most commonly used because of its convenience.

(a) α- particles

Since the range of α- particles in air is relatively

small, all the energy of the α's can be absorbed in the air in a moderately sized cylindrical ion chamber and all ions that are generated can be collected.

These ions can be collected by increasing the voltage across the electrodes of the ion chamber until all of the ions are swept from the gas to the electrodes and the current becomes independent of the applied voltage (saturation current). Fig. I - 2.

If the total ionization can be measured, the energy dissipated in the system can be calculated from the equation:

$$E = J W$$

Where E = energy absorbed by the air in the chamber

J = number of ion pairs produced in the air

W = energy absorbed per ion pair

= 35 eV for α-particles in air.

(b) X- and γ- rays

The ranges of X- and γ-rays are much greater than those of α-particles, therefore the above method cannot be used to measure the total energy of the Compton electrons in a radiated gas. A different type of ionization chamber must be used.

(i) Standard air chamber (free air chamber)

In a standard air chamber, a narrow beam of X-rays is passed between a pair of parallel plate electrodes that are separated sufficiently so that the secondary electrons

FIGURE I - 2

Dependence of the Current Density on the Electric Field

1. Not collecting all electrons and ions generated by α's and secondary electrons.

2. Collecting all ions (saturation current).

3. Secondary electrons are being sufficiently accelerated by the electric field that they can cause further ionization.

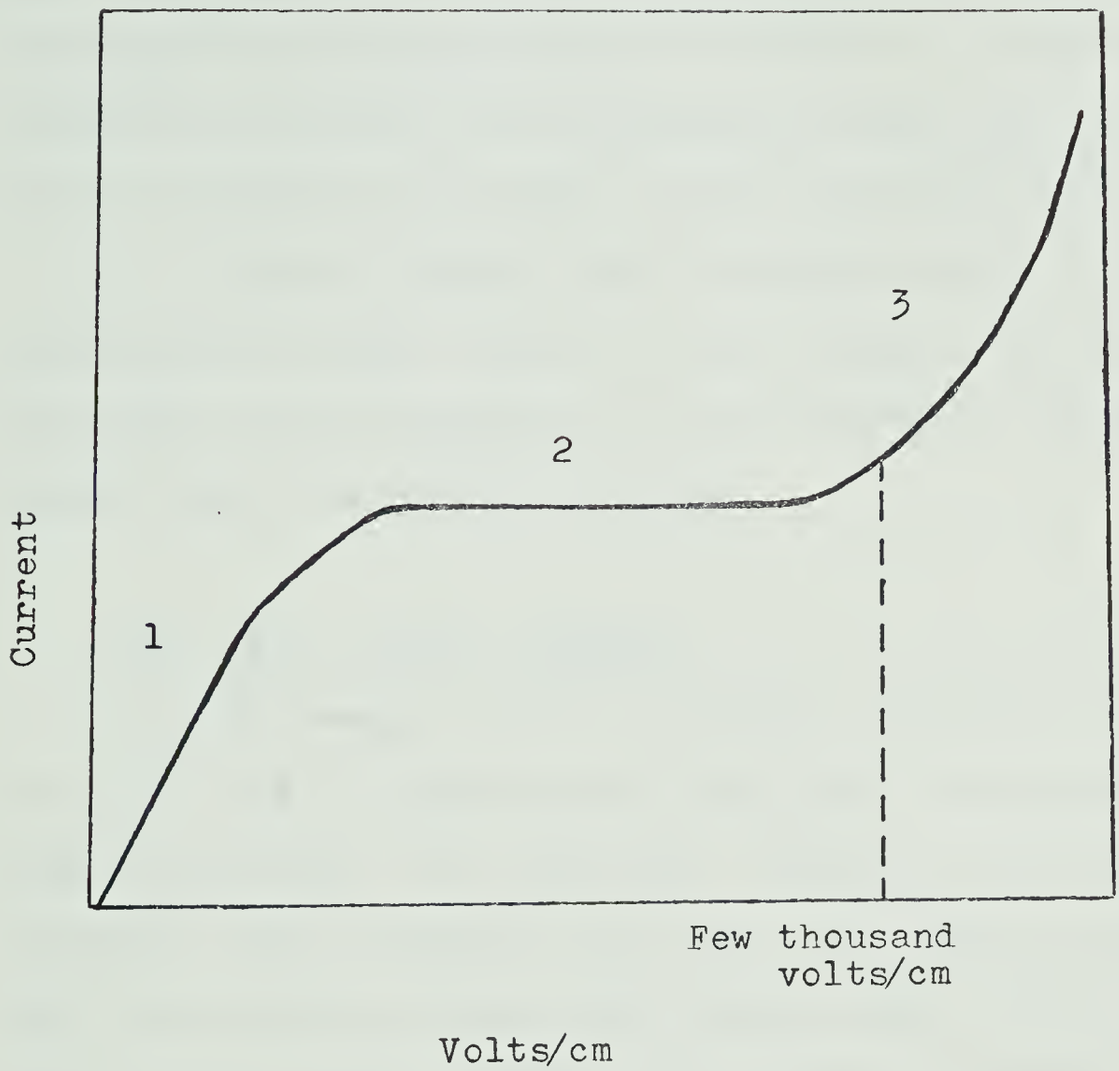
Current
1
2
3
Few thousand
volts/cm
Volts/cm

(electrons set in motion by the electrons which have been generated by the X- or γ- rays) do not reach them in the absence of an electric field. Otherwise, some of the energy of these electrons would be lost in the walls and would not cause ionization in the air between the plates. A guard plate surrounding the collecting electrodes prevents distortion of the electric field at the edges of the collector plate.

The air chamber must be placed at an electrode equilibrium distance (where as many primary electrons are generated as are terminated in any element of volume of the medium) from the radiation source.

(ii) "Air - wall" chambers

The ranges of the secondary electrons for high energy X- and γ- rays are too great for a convenient sized free air chamber. The "air-wall" chambers, designed by Bragg and Gray, which consists of a small air volume enclosed by a wall of a material whose mean atomic number approximates that of air is used instead. Gamma rays interact with the wall material in much the same way as they would with air, and the decrease in the range of the electrons is directly proportional to the increased density of the wall material with respect to air.

The size of the cavity should be such that the secondary electrons lose only a small fraction of their energy in crossing it, and the wall thickness must be greater than the range of the primary electrons in the wall material. A centrally positioned wire within the thimble chamber is charged to a

given potential. When the chamber is irradiated, the charge on the wire is reduced. The decrease in potential gives a measure of the ionization produced by the radiation. An "air-wall" chamber is calibrated with a standard air chamber.

(iii) Radiolysis cells

Gas phase radiolysis cells have been used to measure energy absorbed in much the same way as the two previously mentioned ionization chambers. However, since electronic equilibrium is not established in the wall, the amount of ionization produced in the gas being studied is compared with the amount produced in a standard gas such as air.

6. OBSERVED TEMPERATURE EFFECT ON ION COLLECTION IN RADIOLYSIS CELLS

During the attempt to measure the W-value of methyl-cyclohexane vapour, Holtslander found that the saturation current measured in a cylindrical Pyrex cell (silver film electrode) was temperature dependent (3). Further investigation showed that the saturation currents obtained in air and in ethylene in the cylindrical vessel were also temperature dependent. Similarly, Jones and Sworski (4), while examining the effect of temperature on nitrous oxide radiolysis in stainless steel cylindrical cells, observed that at a given density of nitrous oxide, the change in the saturation current observed on increasing the temperature from 24°C to 200°C was about 15%. This temperature dependence of the saturation

current is not understood, because present knowledge of ionized gases indicates that the saturation current should be independent of temperature in the pressure and temperature range studied by Holtslander and by Jones and Sworski. This will be further discussed later in the thesis. The purpose of the work reported in this thesis was to investigate the cause of the effect of temperature on the saturation current obtained in gas radiolysis cells.

E X P E R I M E N T A L

1. GASES USED FOR RADIOLYSIS

The argon, helium, and hydrogen were obtained from Matheson of Canada Ltd. The argon used was a purified grade of 99,998% min. purity. The helium was a high purity grade of 99.995% min. purity. The hydrogen was an extra dry grade of 99.9% min. purity.

Before being admitted into the conductance cells, the above gases and air were dried by passing them through a cold trap filled with 14-20 mesh Silica Gel immersed in a 95% ethanol slush.

2. RADIOLYSIS CELLS

A. Pyrex Parallel - plate Cell

A wide variety of radiolysis cells were used to measure the saturation currents of the different gases. The largest number of current measurements were taken in 5.08 cm parallel - plate Pyrex cells with the electrodes spaced about 2.54 cm apart (see Fig. II-1A). The metal electrodes all had rolled edges and were of either aluminium or platinium. Aquadag was also used. About three indentations were pushed through the Pyrex wall to help hold each metal electrode in place. Thus in cells of this design there was contact at several points between the walls and the electrodes.

Parallel-plate cells with 2.54 cm diameter aluminium

FIGURE II - 1

Cells for Measurements of Saturation Currents

A. Pyrex Parallel-plate Cell

B. Pyrex Parallel-plate Cell with Guard Ring

C. Pyrex Parallel-plate Cell with Kovar Section

Scale 1 cm = 1 cm

A

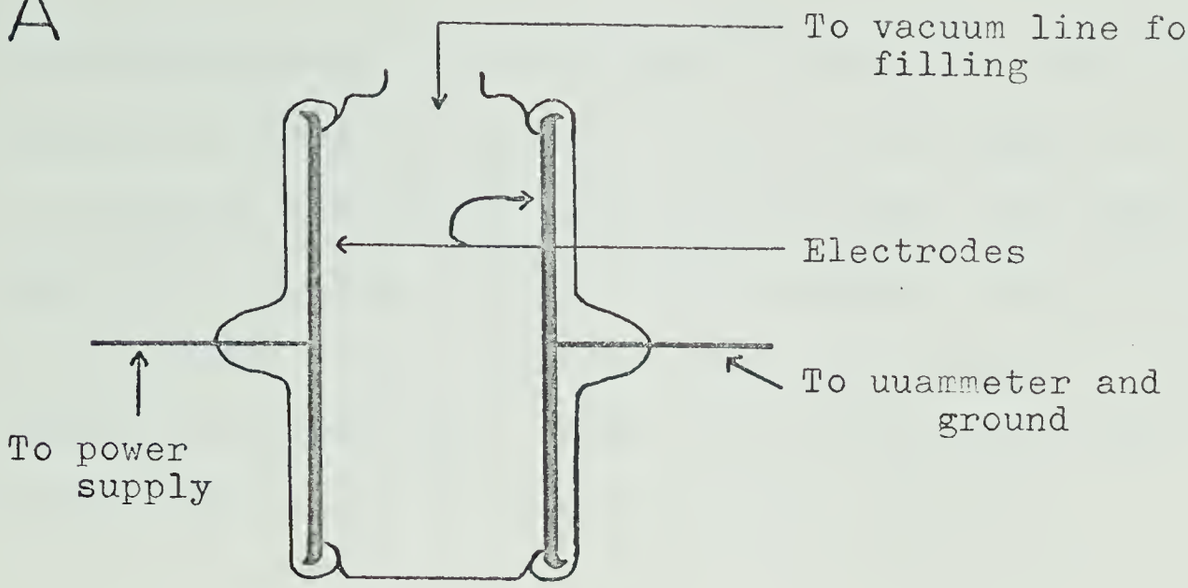
To vacuum line for filling
Electrodes
To uuammeter and ground
To power supply

B

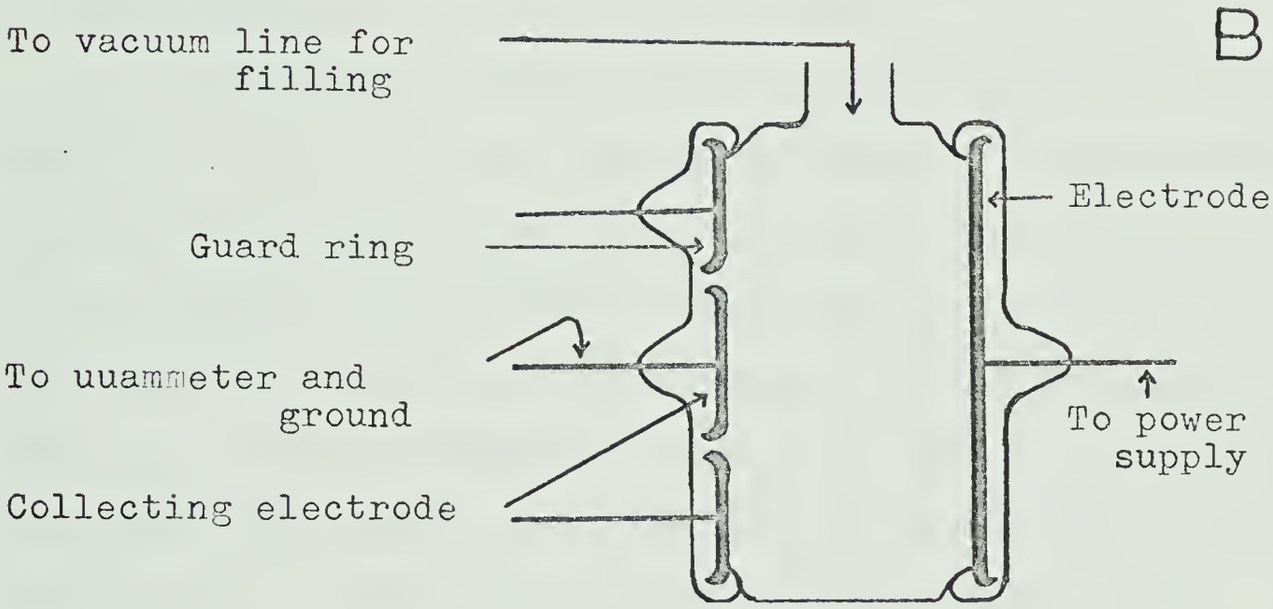
To vacuum line for filling
Electrode
Guard ring
To uuammeter and ground
To power supply
Collecting electrode

C

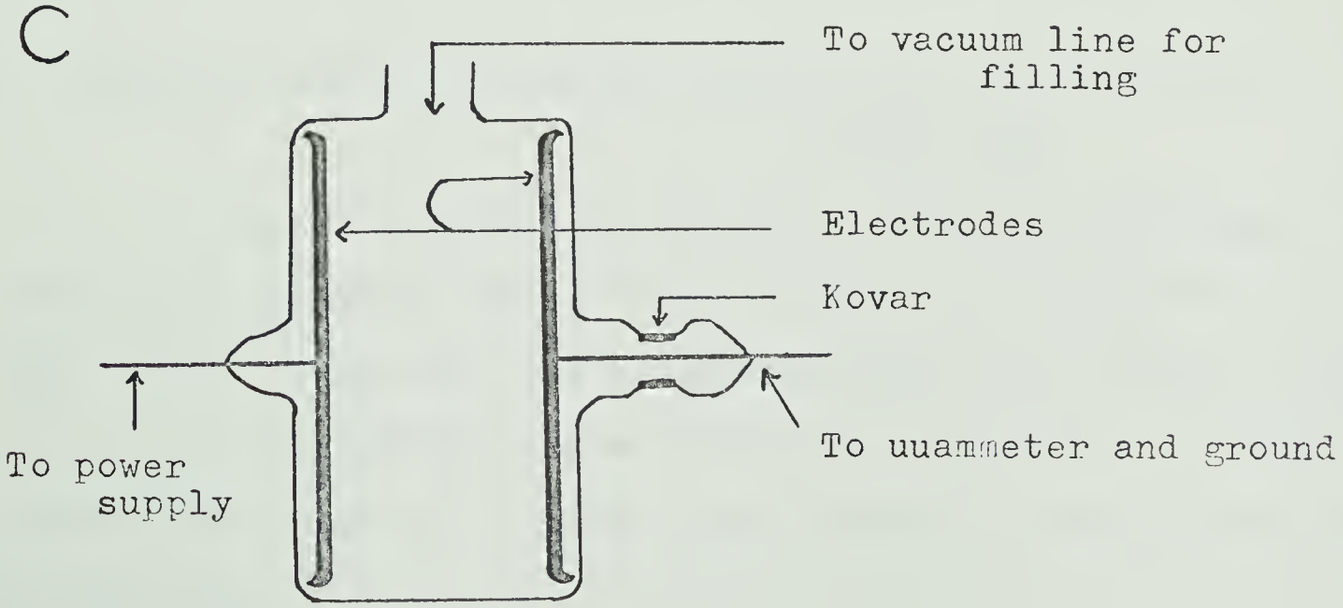
To vacuum line for filling
Electrodes
Kovar
To power supply
To uuammeter and ground

electrodes spaced 1.1, 2.3, and 7.3 cm apart; 5.08 cm aluminium electrodes spaced 1.1 and 2.3 cm apart; and 7.62 cm aluminium electrodes spaced 2.8 cm apart were used to study the temperature effect on saturation currents as a function of the ratio of the diameter of the electrodes to the distance between the electrodes. These cells were constructed the same as the ones described in the previous paragraph.

B. Parallel-plate Cell with Guard Ring

To obtain a more uniform electric field in the region of ion collection a parallel-plate cell with a 1.80 cm diameter collecting (platinium) electrode surrounded by a 1.45 cm wide guard ring was made. These were 0.10 cm apart and were spaced 2.9 cm from a high voltage platinium electrode that was 4.8 cm in diameter. The guard ring and high voltage electrode made contact with the wall at the points of the indentations. This cell is illustrated in Fig. II-1B.

C. Parallel-plate Cell with a Kovar Section in the Stem of the Cell

A parallel-plate cell with aluminium electrodes, 5.08 cm in diameter spaced 2.54 cm apart, was designed as in Fig. II-1C. This cell had no indentations and therefore there was no contact between the wall and the electrodes. A Kovar section, one-half cm in width, was inserted in one of the stems of the cell.

D. Parallel - plate Cell with Aluminium Electrodes that Did Not Touch the Walls

A Pyrex cell with 4.7 cm diameter aluminium electrodes, 2.15 cm apart, similar to the cell in Fig. II-1C but without a Kovar section in the stem was made. Thus in this cell, there also was no contact between the walls and the electrodes.

E. Pyrex Spherical Cell

A Pyrex spherical cell with an outside 6.1 cm diameter and a 1.1 cm diameter aluminium sphere supported in the center by a glass-covered tungsten rod was constructed as shown in Fig. II-1A. The inside of the sphere was painted with aquadag.

F. Conducting Plugs

All the conducting plugs used in the experimental work were designed as in Fig. II-2B. The quartz and glass tubings were heated in the center until an approximately one cm solid plug formed. Tungsten stems were placed about 2 mm apart in the solid part of the plug. The final length of the device was 6 cm. The ceramic plugs were of approximately the same dimensions.

G. Ceramic Cell

A parallel-plate radiolysis cell (see Fig. II-3A) was constructed with stainless-steel electrodes, and a partial

FIGURE II - 2

Spherical Cell and Conducting Plug

A. Pyrex Spherical Cell

B. Pyrex Conducting Plug

Scale 1 cm = 1 cm

A

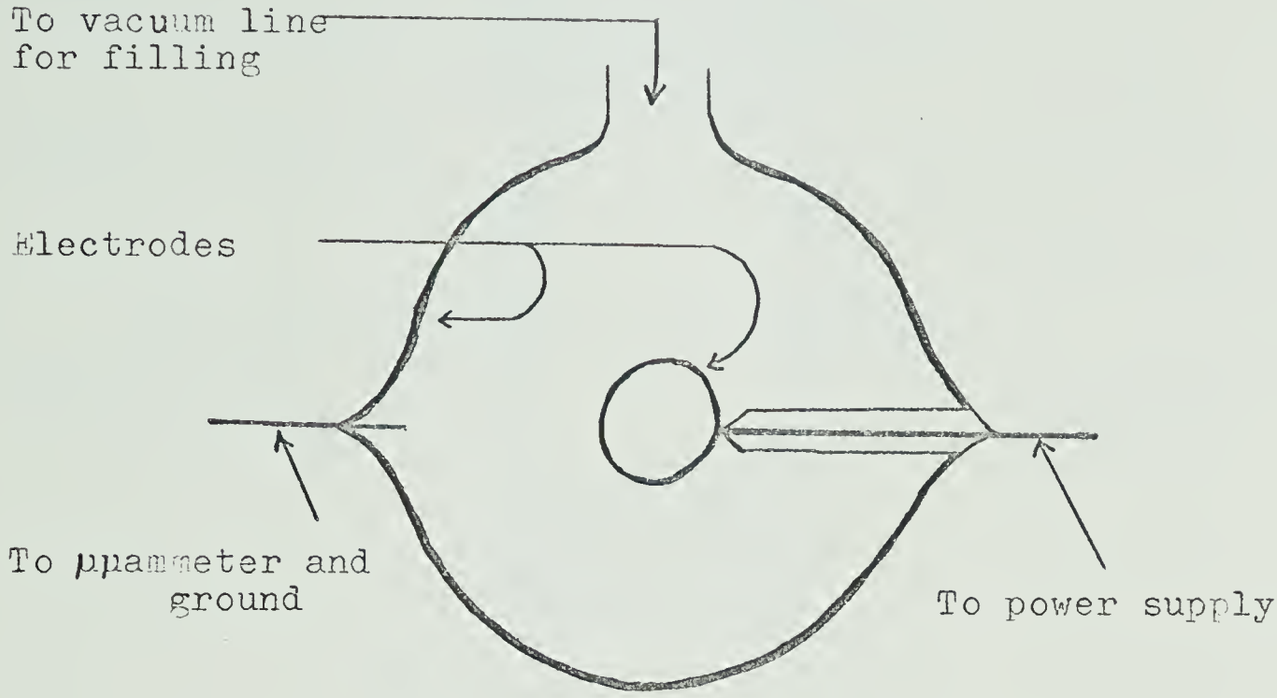
To vacuum line for filling
Electrodes
To μμammeter and ground
To power supply

B

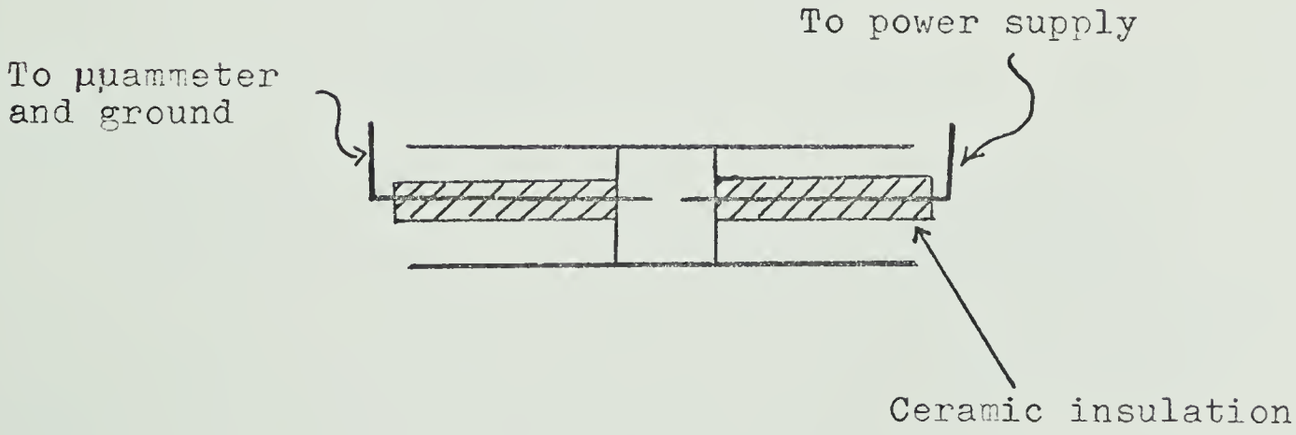
To power supply
To μμammeter and ground
Ceramic insulation

FIGURE II - 3

Radiolysis Cells

A. Ceramic Cell

B. Stainless - steel Spherical Cell

Scale 1 cm = 1 cm

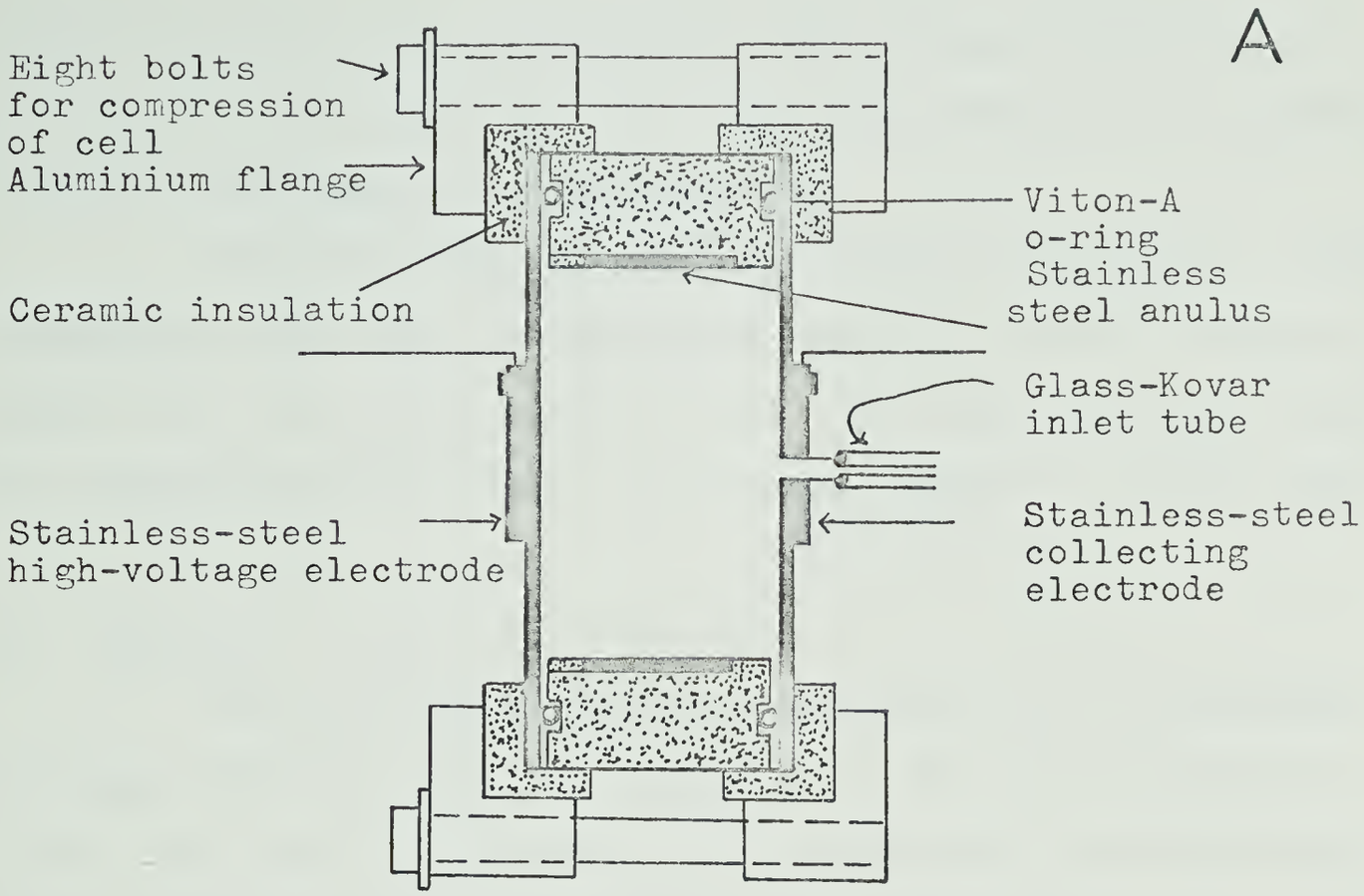
A
Eight bolts for compression of cell
Aluminium flange
Ceramic insulation
Viton-A o-ring
Stainless steel anulus
Glass-Kovar inlet tube
Stainless-steel high-voltage electrode
Stainless-steel collecting electrode

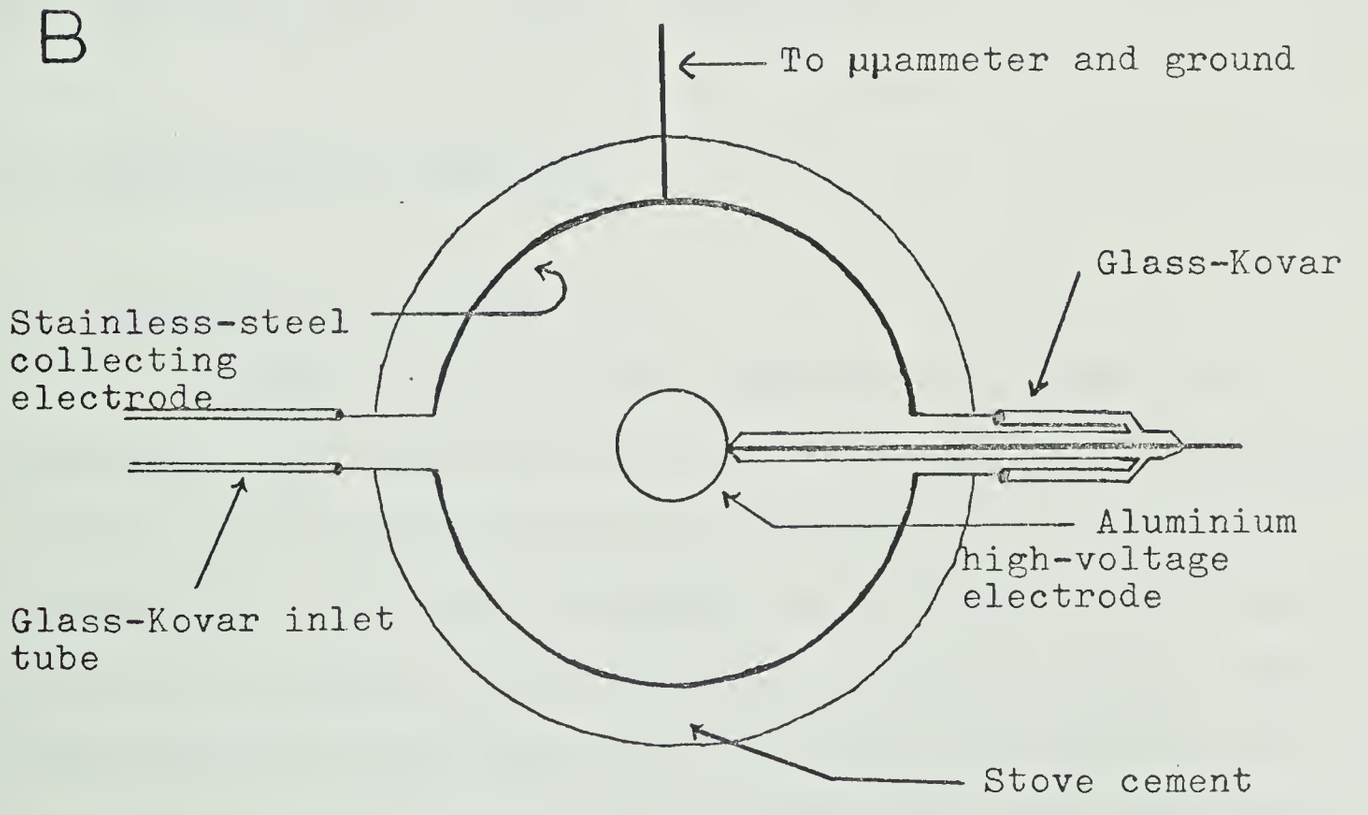
B
To μμammeter and ground
Glass-Kovar
Stainless-steel collecting electrode
Aluminium high-voltage electrode
Glass-Kovar inlet tube
Stove cement

stainless-steel wall. Supra-Mica 500 ceramic insulated the electrodes from the wall. The resultant cavity was a cylinder 2.54 cm long with a 4.5 cm diameter.

Several cells of similiar design with various ceramic insulation were made but none were used for current measurements as it was not possible to make one that was vacuum tight. It was difficult to obtain an airtight rubber to ceramic seal.

H. Stainless - steel Spherical Cell

The 305 stainless-steel spherical cell, illustrated in Fig. II-3B was parallel in design to the Pyrex spherical cell. The cell was coated on the outside with an insulating stove cement (Sairset High Temperature Bonding Mortar, Manufactured by A. P. Green, Edmonton).

3. PREPARATION OF SAMPLES

A. Preparation of Cells

After the cells with aluminium electrodes were assembled, the black oxide that had accumulated on the electrode surface during glassblowing was partially removed with hot nitric acid. The cell was rinsed by filling it four times with tap water and four times with doubly distilled water. The cells with platinium electrodes, and the Pyrex cells before the ends were painted with Aquadag were cleaned with hot sulfonitric acid, and rinsed as above.

The cells were thoroughly baked under vacuum at

360°C - 400°C for about four hours before their initial use and before each experiment. In the initial baking of the cells with Aquadag electrodes, at 300°C, a tarry material slowly distilled out. After the first several hours of baking, no further material was evolved.

B. Filling of the Cells

After the cells were baked out in the vacuum line (see Fig. II - 4) for 3 - 4 hours, they were cooled to room temperature and then flushed out several times with the gas that was to be irradiated. These gases were bubbled into the filling system through mercury, passed through a U-trap filled with Silica Gel and surrounded by 95% ethanol slush, and then the ionization cells were sealed off. The gas pressures in the cell were measured with a mercury manometer. The room temperature during the time that the cells were filled was recorded.

4. IRRADIATION OF THE SAMPLES

The radiolysis cells and conductance plugs were irradiated in a 12,300 curie Gammacell 220 and at a variable distance from a 5000 curie cobalt-60 source. Both sources were obtained from Atomic Energy of Canada Ltd.

Heating of the cells was accomplished by means of a heating mantle made from electrical heating tape. The temperature was regulated by means of a D.C. variable transformer, and was measured with an iron-constantan thermocouple which was placed between the cell and the heating mantle.

FIGURE II-4

Gas Storage and Radiolysis Cell Filling System

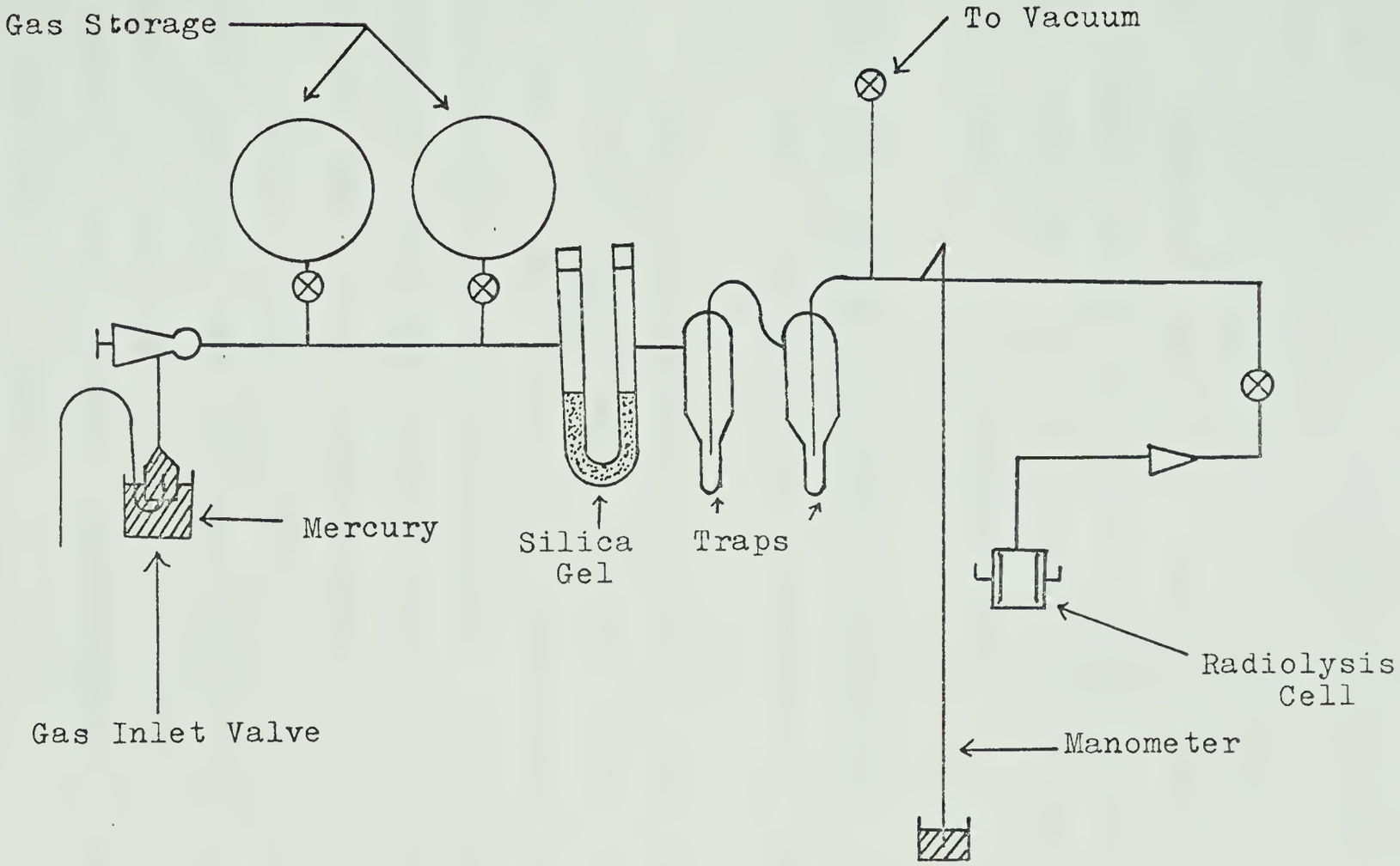
Gas Storage
To Vacuum
Mercury
Silica Gel
Traps
Radiolysis Cell
Gas Inlet Valve
Manometer

The cells were placed in an aluminium stand which could be reproducibley positioned in the drawer of the Gamma-cell source or placed at any variable,reproducible distance from the 5000 curie cobalt-60 source.

Electrical and thermocouple leads were brought to the cell through the top of the Gammacell. From the 5000 curie cobalt-60 source, the coaxial cables and thermocouple leads were suspended from the ceiling and followed the entrance maze from the cave into an adjacent lab.

5. ELECTRICAL CIRCUIT AND CURRENT MEASUREMENT

The electric circuit is schematically shown in Fig. II-5.

One of the electrodes of cell "C" was connected to a Fluke No. 413C High Voltage D.C. power supply. Currents, in the range, 1×10^{-13} to 1×10^{-4} amperes were measured with an E-H Model 240 Micromicroammeter. The Micromicroammeter was calibrated with known currents obtained by placing a known resistance across a known voltage supply.

Current-voltage measurements in the absence of gamma radiation indicated that the blank currents were mostly due to dielectric loss from the cables, or pickup of currents by the cables from stray fields. Blank values of (i/v) were usually less than 10^{-12} mho.

Current-voltage measurements taken while the cell was heated were taken with the D.C. power supply for the heating mantel turned off. The D.C. power supply induced a current

FIGURE II-5

Electrical Circuit

D.C. is the source of direct current voltage

C is the electrolytic cell

I is a current-measuring device

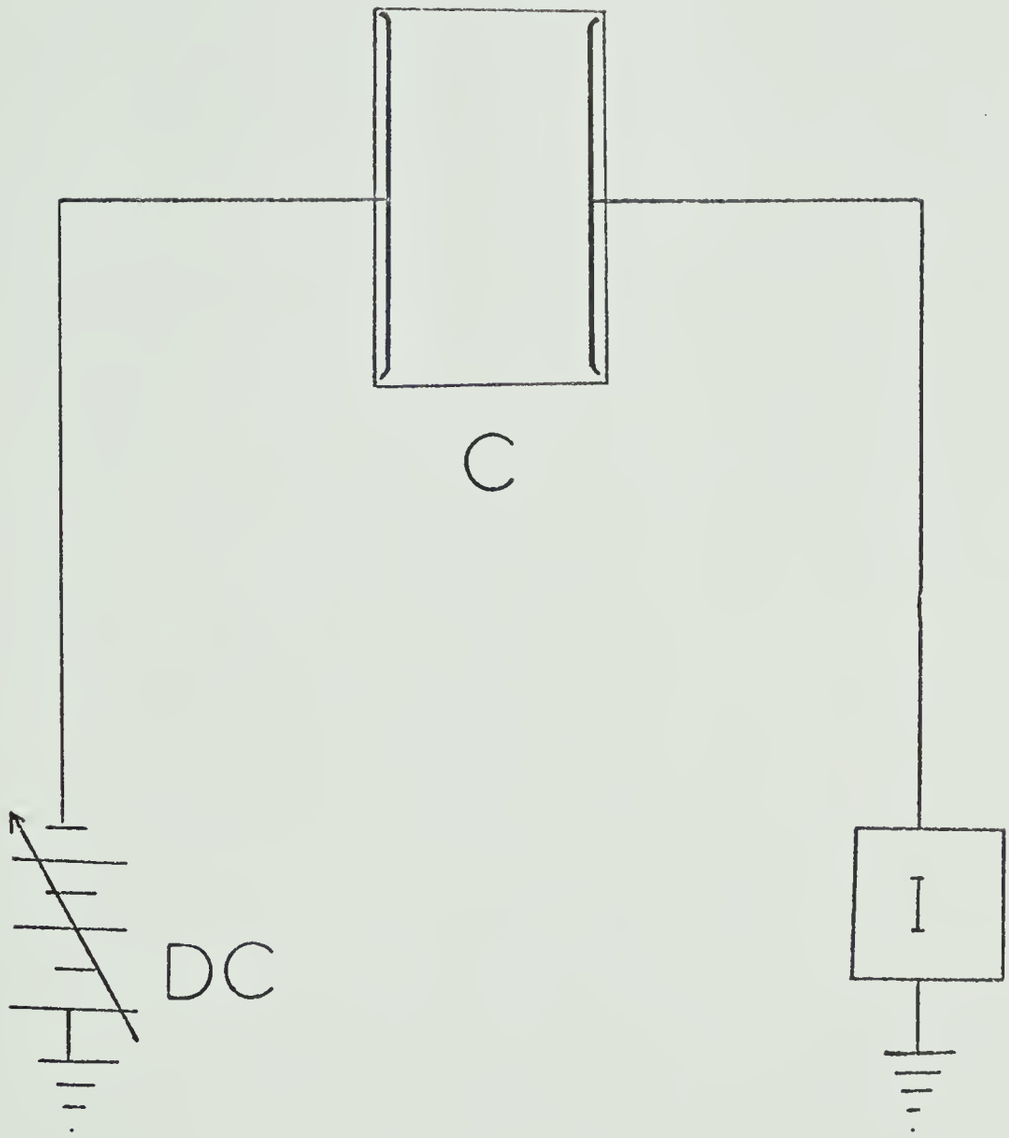
C
DC
I

in the circuit, the sign of which depended upon the direction of flow of current, and the size upon the voltage of the power supply.

R E S U L T S

1. PYREX RADIOLYSIS CELLS

A. Temperature Effect in Different Gases - Parallel-plate Electrodes

The saturation currents for air, argon, helium and hydrogen were measured in a cell (Fig. 11-1A) with 5.08 cm aluminium electrodes spaced 2.54 cm apart. The voltage supply and electrometer were connected to the parallel-plates, the cell was irradiated, and current measurements were taken at varying temperatures from -196°C to +170°C. The gas density was constant as the temperature was varied because the cells were sealed. Reproducible saturation currents were obtained at room temperature, but reproducibility decreased with increasing temperature.

With an initial pressure of about 300 torr and an initial temperature of around 25°C, the saturation currents for the four gases were lowered by temperature increases above 50°C and up to approximately 110°C, above which temperature good saturation current measurements could not be made. When current measurements were taken outside of the radiation beam, it was found that significant background currents began appearing at approximately 110°C, i.e. at the temperature where good plateaus began disappearing. The percent decrease in the saturation currents from 25°C to 80°C and 110°C are presented in Table III - 1.

TABLE III - 1

Temperature Effect on Saturation Currents *

Gas	Ave. No. Electrons Per Mol.	Temp. (°C)	Saturation Current (Positive)	Decrease from 25°C	Per Cent Decrease
H_2	2.0	25	1.6×10^{-7}		
		80	1.3×10^{-7}	2.7×10^{-8}	17.2
		110	8.5×10^{-8}	7.2×10^{-8}	45.8
He	2.0	25	1.2×10^{-7}		
		80	1.1×10^{-7}	1.0×10^{-8}	8.3
		140	8.9×10^{-8}	3.2×10^{-8}	26.4
Air	14.4	25	10.0×10^{-7}		
		80	9.3×10^{-7}	8.0×10^{-8}	7.9
		110	7.9×10^{-7}	2.2×10^{-7}	21.8
Argon	18	25	14.0×10^{-7}		
		80	12.9×10^{-7}	1.0×10^{-7}	7.4
		110	11.6×10^{-7}	2.4×10^{-7}	17.4

* Pyrex cell with Al. electrodes.

The background and net positive currents for each of the gases at the different temperatures are shown in Figures III-1, III-2, III-3, and III-4. The negative currents were almost the same as the positive currents for all the gases.

TABLE III - 1

Temperature Effect on Saturation Currents *

Gas	Ave. No. Electrons Per Mol.	Temp. (°C)	Saturation Current (Positive)	Decrease from 25°C	Per Cent** Decrease
H_2	2.0	25	1.6×10^{-7}		
		80	1.3×10^{-7}	2.7×10^{-8}	17.2
		110	8.5×10^{-8}	7.2×10^{-8}	45.8
He	2.0	25	1.2×10^{-7}		
		80	1.1×10^{-7}	1.0×10^{-8}	8.3
		140	8.9×10^{-8}	3.2×10^{-8}	26.4
Air	14.4	25	10.0×10^{-7}		
		80	9.3×10^{-7}	8.0×10^{-8}	7.9
		110	7.9×10^{-7}	2.2×10^{-7}	21.8
Argon	18	25	14.0×10^{-7}		
		80	12.9×10^{-7}	1.0×10^{-7}	7.4
		110	11.6×10^{-7}	2.4×10^{-7}	17.4

* Pyrex cell with Al. electrodes.

** Reproducable within about 10% of the per cent decrease.

The background and net positive currents for each of the gases at the different temperatures are shown in Figures III-1, III-2, III-3, and III-4. The negative currents were almost the same as the positive currents for all the gases.

FIGURE III-1

Currents Measured in Pyrex Cell with Aluminium Electrodes

Air: Pressure at 25°C = 305 torr

Density = 0.475×10^{-3} gm/cm^3

A. Background Current

▽ : 140°C

● : 170°C

In addition, the following background currents were measured.

25°C : 1×10^{-9} amps at +3000 V

80°C : 1.5×10^{-9} amps at +3000 V

110°C : 0.13×10^{-7} amps at +3000 V

B. Net Positive Current

○ : 25°C

□ : 80°C

△ : 110°C

▽ : 140°C

● : 170°C

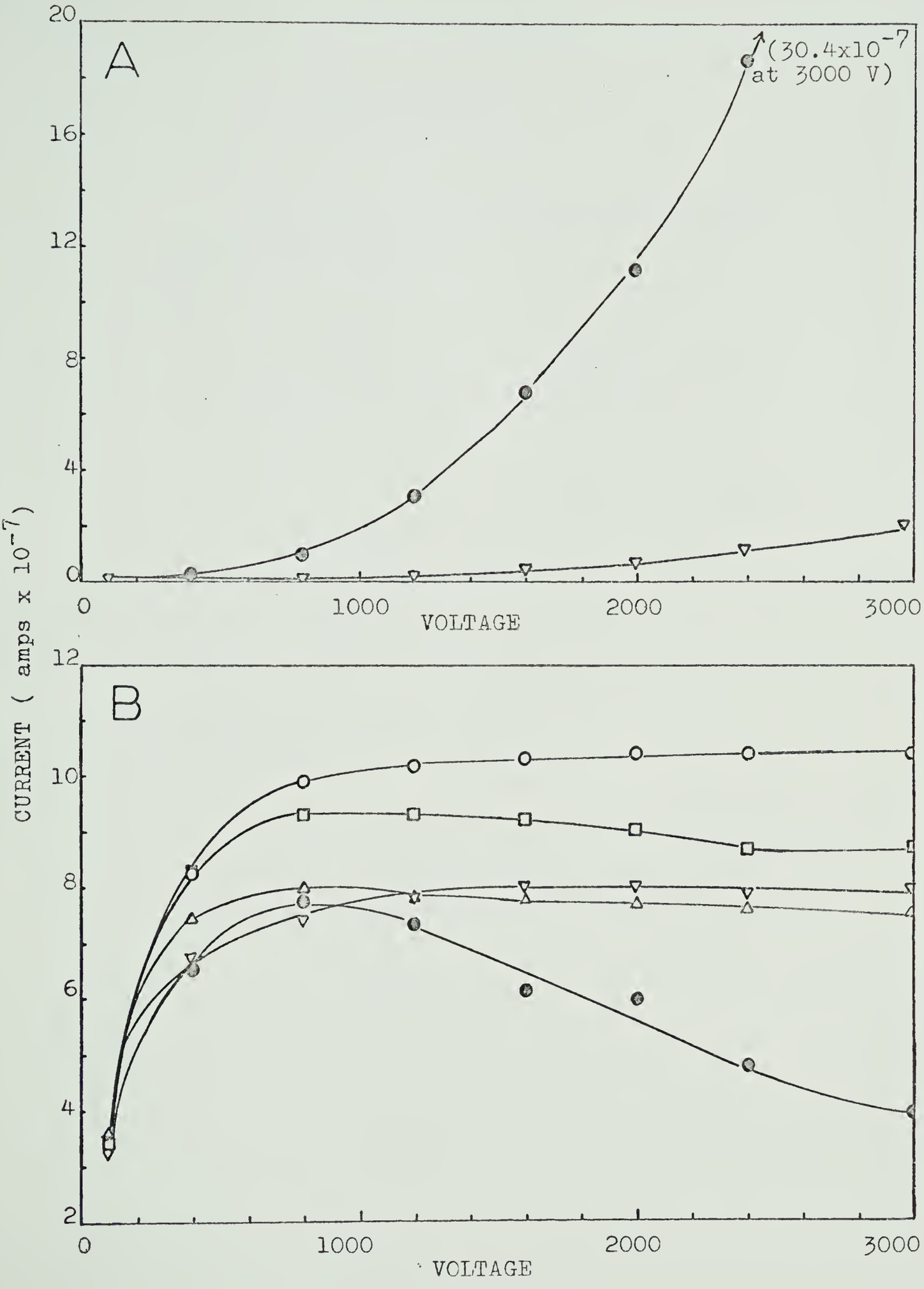
A
(30.4x10^-7 at 3000 V)
20
16
12
8
4
0
0
1000
2000
3000
VOLTAGE
B
12
10
8
6
4
2
0
1000
2000
3000
VOLTAGE
CURRENT (amps x 10^-7)

FIGURE III-2

Currents Measured in Pyrex Cell with Aluminium Electrodes

Argon: Pressure at 25°C = 299 torr

Density = 0.643×10^{-3} gm/cm^3

A. Background Current

▽ : 140°C

● : 170°C

In addition, the following background currents were measured.

25°C : 0.42×10^{-9} amps at +3000 V

80°C : 0.46×10^{-8} amps at +3000 V

B. Net Positive Current

○ : 25°C

□ : 80°C

△ : 110°C

▽ : 140°C

● : 170°C

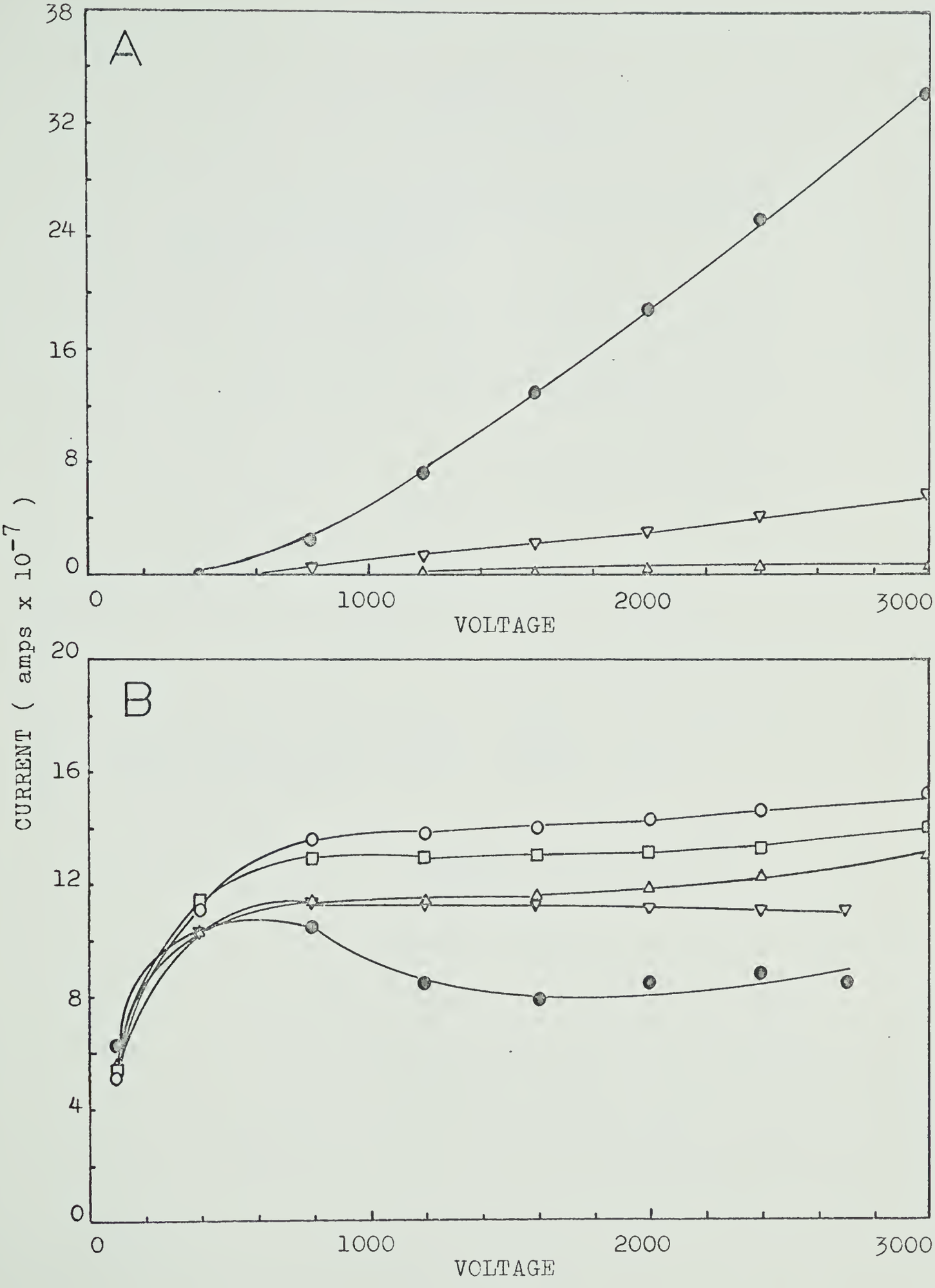
A
38
32
24
16
8
0
0
1000
2000
3000
VOLTAGE
CURRENT (amps x 10^{-7})
B
20
16
12
8
4
0
0
1000
2000
3000
VOLTAGE

FIGURE III-3

Currents Measured in Pyrex Cell with Aluminium Electrodes

Helium: Pressure at 23°C = 280 torr

Density = 0.606×10^{-4} gm/cm^3

A. Background Current

▽ : 140°C

● : 170°C

In addition, the following background currents were measured.

25°C: 1.30×10^{-11} amps at +1400 V

110°C: 2.10×10^{-9} amps at +1400 V

B. Net Positive Current

○ : 25°C

□ : 110°C

▽ : 140°C

● : 170°C

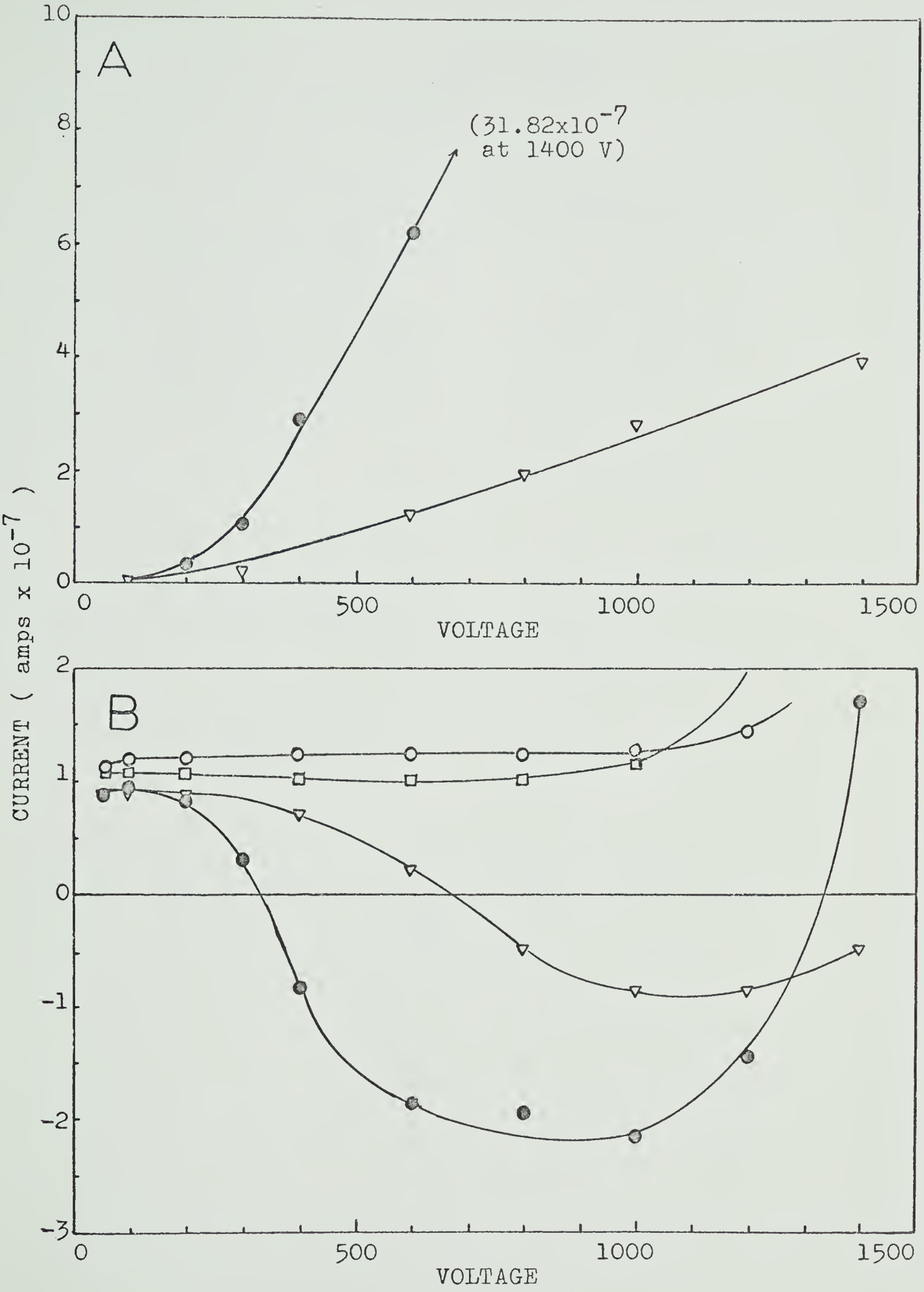
A
(31.82x10^-7 at 1400 V)
10
8
6
4
2
0
0
500
1000
1500
VOLTAGE
B
CURRENT (amps x 10^-7)
2
1
0
-1
-2
-3
0
500
1000
1500
VOLTAGE

FIGURE III-4

Currents Measured in Pyrex Cell with Aluminium Electrodes

Hydrogen: Pressure at 25°C = 299 torr

Density = 0.0324×10^{-3} gm/cm^3

A. Background Current

▽ : 140°C

● : 170°C

In addition, the following background currents were measured.

25°C : 1.0×10^{-11} amps at +3000 V

80°C : 0.4×10^{-8} amps at +3000 V

B. Net Positive Current

○ : 25°C

□ : 80°C

△ : 110°C

▽ : 140°C

● : 170°C

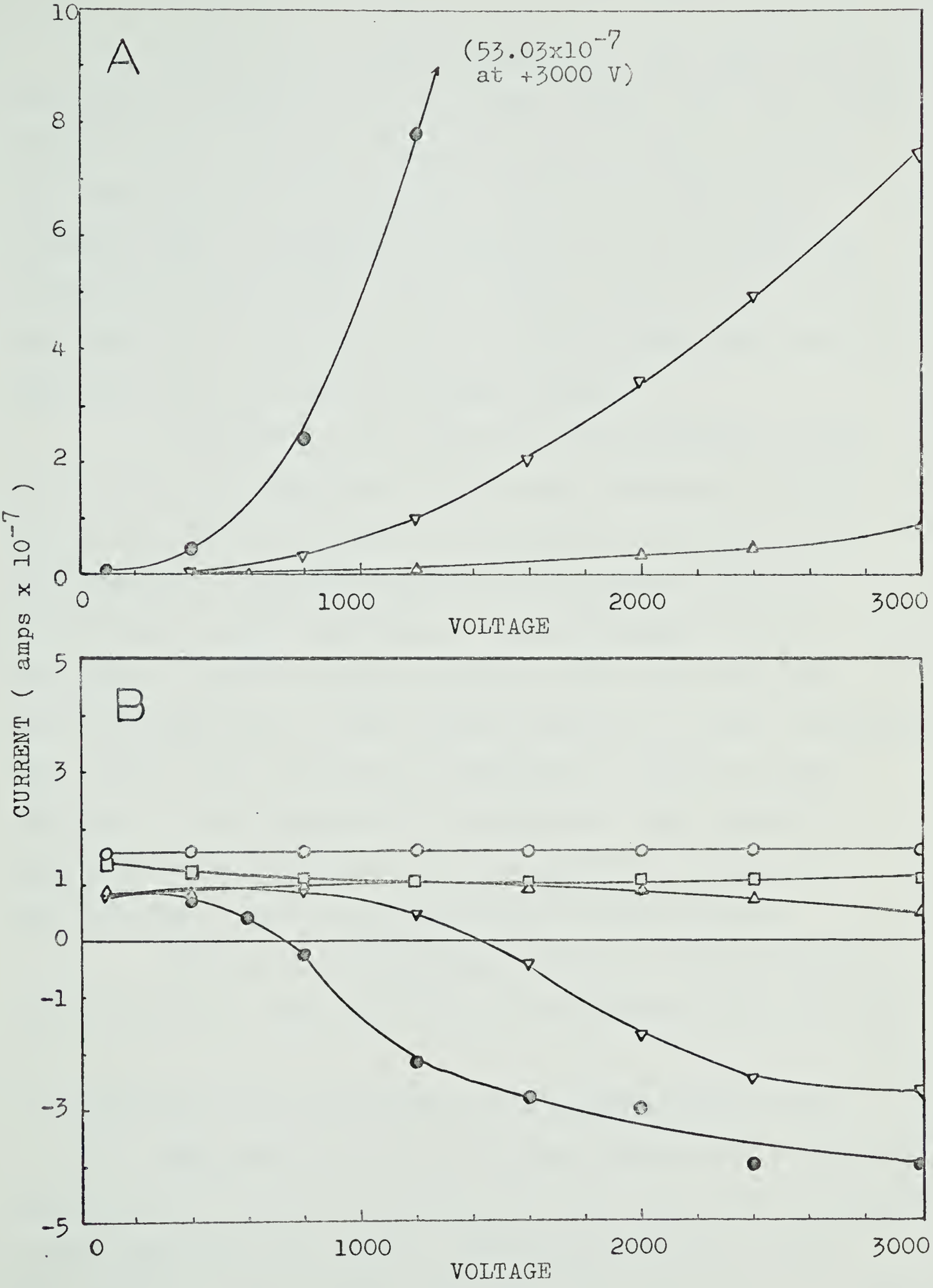
A
(53.03x10^-7
at +3000 V)
10
8
6
4
2
0
0
1000
2000
3000
VOLTAGE
B
5
3
1
0
-1
-3
-5
0
1000
2000
3000
VOLTAGE
CURRENT (amps x 10^-7)

Saturation current measurements were taken for air at initial pressures of 50, 150, 300 and 600 torr and it was found that the percent decrease in the saturation current was independent of the pressure. The voltage per unit pressure that was required to reach current saturation was found to be proportional to the square root of the pressure. The saturation currents for air at 25°C for 50, 150, 300 and 590 torr are illustrated in Figure III-5B.

To determine the effect on the saturation current of lowering the temperature of the gas, readings of the saturation current were taken in the parallel-plate cell with the aluminium electrodes with the cell immersed first in cyclohexane at 25°C and then in liquid nitrogen (liquid nitrogen at -196°C and cyclohexane at 25°C have the same electron densities). The voltage required to attain saturation was greater when the cell was immersed in liquid nitrogen than when it was immersed in cyclohexane. This effect became less pronounced as the initial pressure of the air was decreased. This is illustrated in Figure III-5B.

There was no temperature effect on the saturation current when the cell was filled with helium(see Fig. III-5A).

B. Different Electrode Materials in Parallel-Plate Cells

When saturation currents were measured in a parallel-plate cell of the same dimensions but with platinium electrodes, it was found that the initial saturation currents for the four gases were much higher than the ones produced in the cell

FIGURE III - 5

Currents Measured in Pyrex Cell with Aluminium Electrodes

A. Saturation Currents for Helium at 25° and -196°C

Pressure at 23.8°C = 298 torr

Density = 5.89×10^{-5} gm/cm^3

○ : 25°C cell in heating mantel

● : 25°C cell in cyclohexane

△ : -196°C

B. Saturation Currents for Air at 25° and -196°C

○ : 25°C

580 torr; 9.04×10^{-4} gm/cm^3

● : -196°C; 9.04×10^{-4} gm/cm^3

□ : 25°C

300 torr; 4.68×10^{-4} gm/cm^3

■ : -196°C; 4.68×10^{-4} gm/cm^3

△ : 25°C

50 torr; 7.79×10^{-5} gm/cm^3

▲ : -196°C; 7.79×10^{-5} gm/cm^3

▽ : 25°C

150 torr; 2.34×10^{-4} gm/cm^3

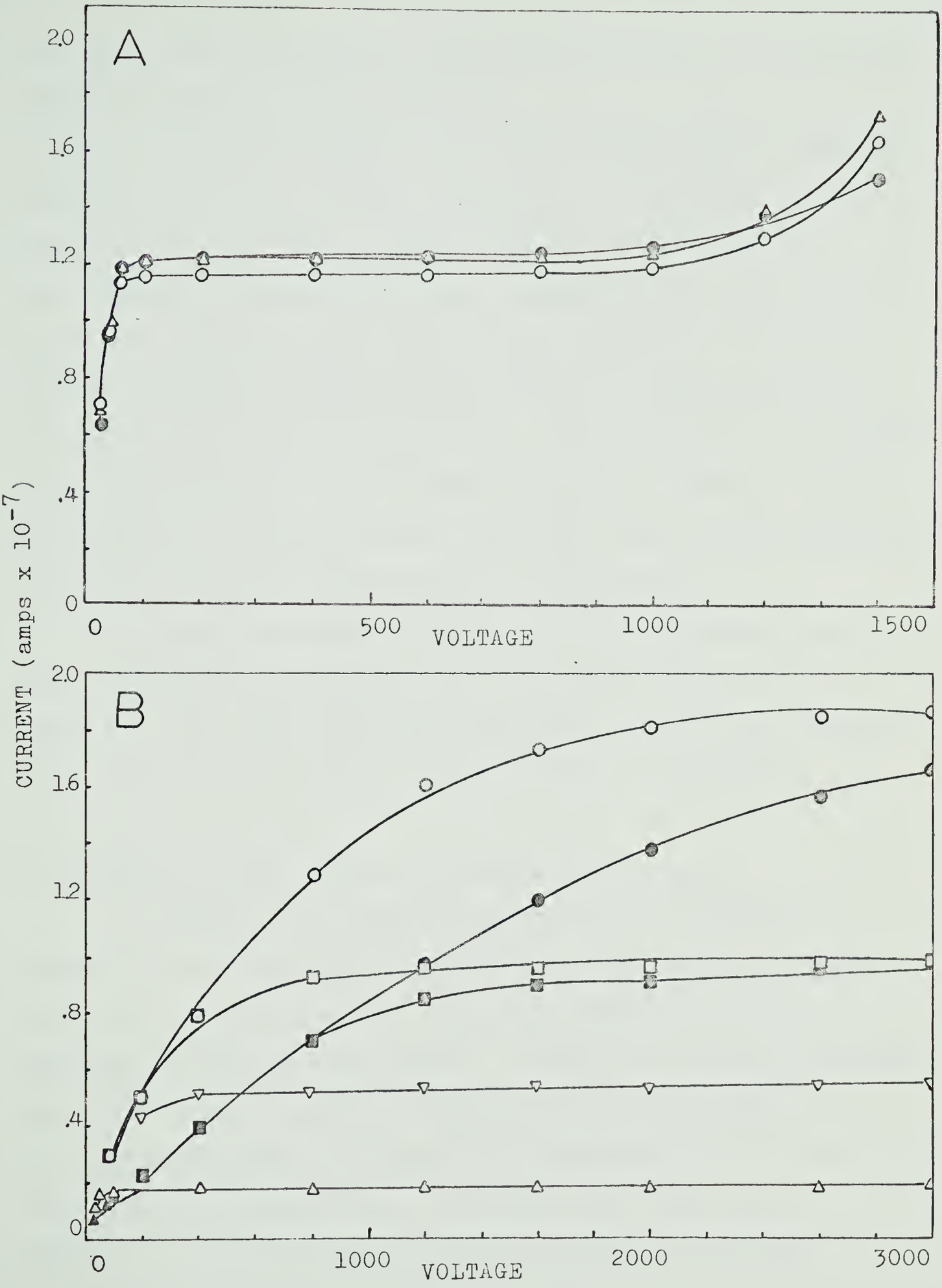
A
2.0
1.6
1.2
.8
.4
0
0
500
1000
1500
VOLTAGE
B
2.0
1.6
1.2
.8
.4
0
0
1000
2000
3000
VOLTAGE
CURRENT (amps x 10^{-7})

with aluminium electrodes. This was attributed to the greater electron density of the platinium.

A cell of similar size with painted aquadag parallel electrodes was used to take measurements of saturation currents in air and argon. The saturation currents at 25°C were almost the same as the ones produced in the cell with aluminium electrodes, but the percent decreases in the saturation currents were more nearly equal to those produced in the cell with platinium electrodes. This cell gave the largest background currents as the temperature was increased. This background current was present even when the cell was evacuated down to a pressure less than 10^{-13} millimeters.

The percentage decreases for the different electrode materials for hydrogen, air and argon are given in Table III - 2. The percentage decreases at 110°C are smaller with the platinium than with the aluminium electrodes.

C. Effect of Guard Rings in Parallel-Plate Cells

Saturation current measurements in a parallel-plate cell with a collecting platinium electrode surrounded by a guard ring (Figure II - 1B) were taken at different temperatures for air and argon. At 80°C, the percent decrease from 25°C in the positive saturation current for air in the cell with guard rings was 8 as compared to 12 in the cell without a guard ring. At 110°C, both cells gave a decrease in the saturation current of about 17 percent.

TABLE III - 2

Effect of Different Electrode Materials on Saturation Currents

Electrode Material	Gas*	Temp. (°C)	Saturation Current (Amps)	Decrease from 25°C (Amps)	Percent Decrease
Aluminium	H_2	25	1.57×10^{-7}		
		80	1.30×10^{-7}	0.27×10^{-7}	17.2
		110	0.85×10^{-7}	0.72×10^{-7}	45.8
Platinium	H_2	25	3.1×10^{-7}		
		80	2.7×10^{-7}	0.4×10^{-7}	12.9
		110	2.25×10^{-7}	0.85×10^{-7}	27.4
Aluminium	Air	25	10.1×10^{-7}		
		80	9.3×10^{-7}	0.8×10^{-7}	7.9
		110	7.9×10^{-7}	2.2×10^{-7}	21.8
Aquadag	Air	25	10.4×10^{-7}		
		80	8.97×10^{-7}	1.43×10^{-7}	13.7
		110	8.61×10^{-7}	1.79×10^{-7}	17.2
Platinium	Air	25	16.9×10^{-7}		
		80	15.35×10^{-7}	1.55×10^{-7}	9.2
		110	14.03×10^{-7}	2.87×10^{-7}	17.0
Aluminium	Argon	25	14.01×10^{-7}		
		80	12.98×10^{-7}	1.03×10^{-7}	7.4
		110	11.57×10^{-7}	2.44×10^{-7}	17.4
Aquadag	Argon	25	11.95×10^{-7}		
		80	11.12×10^{-7}	0.83×10^{-7}	6.9
		110	10.31×10^{-7}	1.64×10^{-7}	13.7
Platinium	Argon	25	24.14×10^{-7}		
		80	22.23×10^{-7}	1.91×10^{-7}	7.9
		110	21.15×10^{-7}	2.99×10	12.4

* The pressure of each gas at 25°C was 300 torr

A comparison of the positive saturation currents for argon at 110°C gave an 8% decrease in the cell with guard rings as compared to 13% in the cell without guard rings. The negative saturation current was almost zero up to 1200 volts, at which voltage there occurred an almost sudden increase which made the negative current about 4% larger than the positive current at the same voltage. After the cell was heated and irradiated while a voltage was applied across the electrodes, the negative current increased at the lower voltages. When the current from the guard ring was measured, it was found that the electrons were being collected mainly on the guard ring.

In an attempt to hold the guard ring very nearly at the same potential as the collector, the circuit as drawn in Figure III - 6 was set up. Since the area of the guard ring was about 7 times that of the collector, the resistor positioned in front of the guard ring was approximately 1/7th of the resistor in front of the collector. It was hoped that the two back voltages would be the same. When the current measurements were taken, it was found that at the lower voltages the negative current from the collector was still much lower than the positive current.

The resistance in front of the collector was replaced with a variable resistor. At the different bias voltages, the resistance was decreased until the negative current at the collector was almost equal to the positive current. The millivolt readings on the two digital volt-

FIGURE III - 6

Circuit for Parallel-plate Cell

with Guard Ring

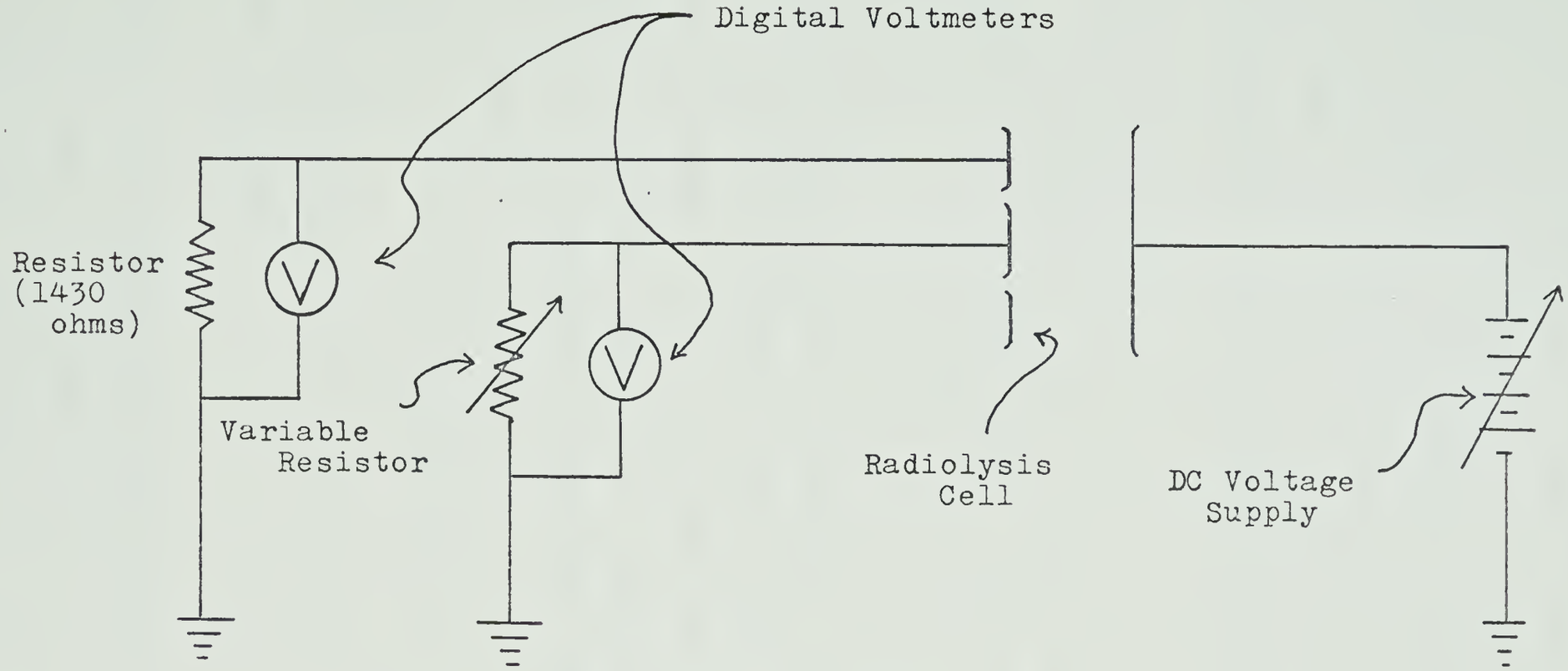
Digital Voltmeters
Resistor
(1430
ohms)
V
Variable
Resistor
V
Radiolysis
Cell
DC Voltage
Supply

meters were recorded. When the difference in the potentials was divided by the distance between the guard ring and the collector, it was found that for up to 1000 volts across the cell, the difference in the potential between the guard ring and the collector was about a half volt per centimeter. For more than 1000 volts across the cell, the voltage difference was zero between the guard ring and the collector.

D. Effect of Conditioning the Cell

The effect of a prior baking of the cell filled with gas and with a voltage applied across the cell (conditioning) on the net hydrogen and helium saturation currents was investigated. When the cells with the parallel platinium and aluminium electrodes were previously baked for several hours with an applied positive bias voltage of 2000, and filled with hydrogen it was found that the net currents were considerably less sensitive to temperature. A comparison of the net currents for hydrogen taken in the cell with the aluminium electrodes with and without previous conditioning is illustrated by comparing Fig. III - 4B with Fig. III - 7A.

Conditioning the cell had no effect on the helium net currents.

E. Cleaning and Grounding the Outer Surface of the Cell

In these experiments a Pyrex cell with 4.7 cm diameter electrodes, 2.15 cm apart was used. In this cell

there was no contact between the walls and the electrodes.

To determine if the large background currents that were present at the higher temperature when the gas was not being irradiated was due to leakage currents along the outside surface of the cell, the cells were thoroughly cleaned on the outside with 95% alcohol. This greatly reduced the background currents in the cells with aluminium and platinium electrodes, but not appreciably in the cell with the painted aquadag electrodes.

To further investigate the cause of the background currents, the outer surface of the cell around the collecting electrode was painted with aquadag and grounded with a copper wire. This reduced the measured background currents to the extent that they were almost negligible compared to the ionized gas currents at all the temperatures. However, at the same time the saturation currents at the higher temperatures also decreased. Different surface areas of the cell were painted with aquadag and grounded. It was found that the larger the surface area that was painted, the smaller were the background currents and the greater were the percentage decreases in the saturation currents from 25°C to 140°C. This is illustrated in Figure III - 7B.

The saturation current at 110°C for an initial pressure of 300 torr of air decreased by 1.5 times the amount when the outside cylindrical part of the cell was painted with aquadag and grounded as compared to when it was not grounded. The decrease of the positive saturation current for air,

hydrogen, and helium at voltages less than about 600 was of the order of 10% to 100% greater than that of the negative saturation current. The percent decrease of the saturation currents, and the greater decreases in the positive current than the negative current for hydrogen was more prominent at the lower pressure (see Fig. III - 8A, 8B). In air, the percent temperature effects were independent of pressure (see Fig. III - 8C, 8D) as in the ungrounded cell.

A Kovar section was inserted in the stem of a Pyrex cell midway between the collecting electrode and the point where the tungsten lead from the collecting electrode terminated with an electrical connecter (Fig. III - IC). It was hoped that by grounding the Kovar section, any leakage currents along the inside and the outside of the Pyrex surface could be eliminated. Grounding the Kovar section had no effect on the background currents.

F. Variation of d/l for Cell with Parallel Plate Aluminium Electrodes

The geometry for the parallel-plate electrode cells was varied and saturation current measurements for air, hydrogen, and helium were taken at various temperatures while the outer surface of the cells around the collecting electrode was grounded. In general, as the ratio of the diameter of the electrode (d), to the distance between the electrodes (l), decreased, the percent decrease in the sat-

FIGURE III-7

Currents Measured in Pyrex Cell with Aluminium Electrodes

A. Net Currents in Hydrogen in a Conditioned Cell

(see currents in an unconditioned cell on p. 35)

- ○ : 25°C
- □ : 80°C
- ▽ : 140°C
- ◐ : 180°C

B. Net Currents in Air When Different Surface Areas of Pyrex Cell Were Painted with Aquadag and Grounded

- ○ : Saturation current for 300 torr of air at 25°C
- □ : Net current at 140°C
- △ : Saturation current at 140°C when center half of outer end surface of cell near collecting electrode was painted with aquadag and grounded
- ▽ : Saturation current at 140°C when outer surface of cell around collecting electrode was painted with aquadag and grounded
- ● : Saturation current at 140°C when entire side surface of cell was painted with aquadag and grounded

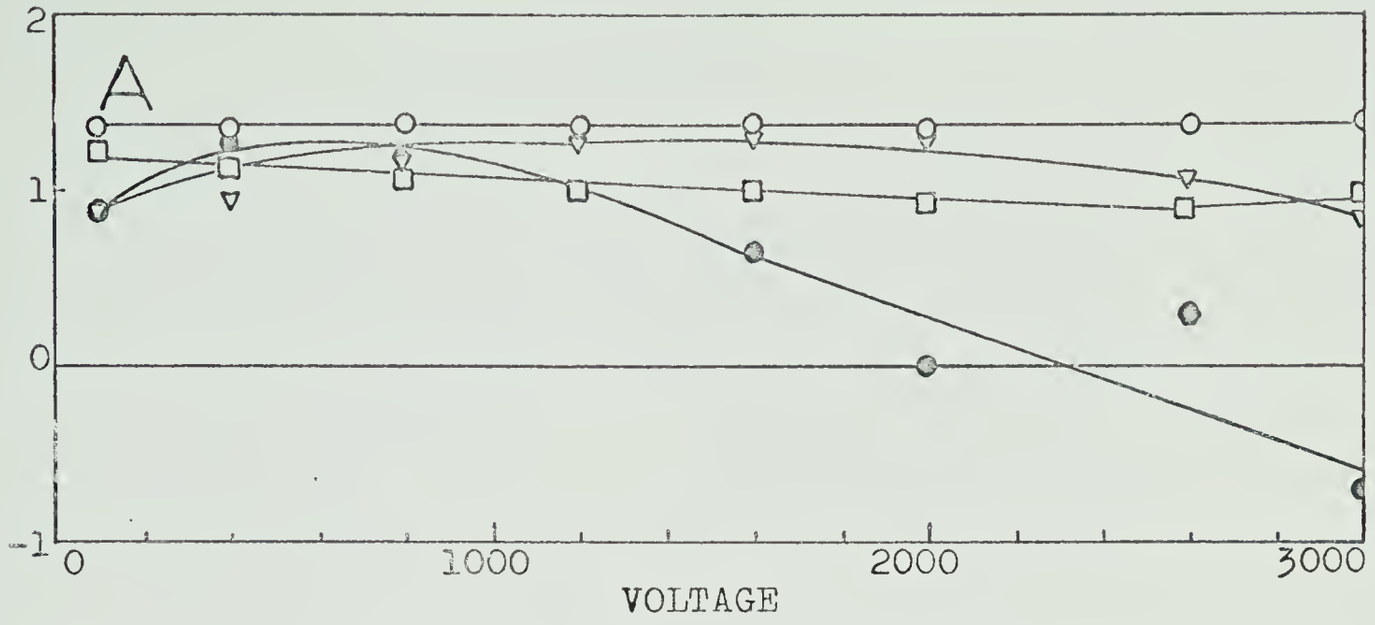
A
2
1
0
-1
0
1000
2000
3000
VOLTAGE

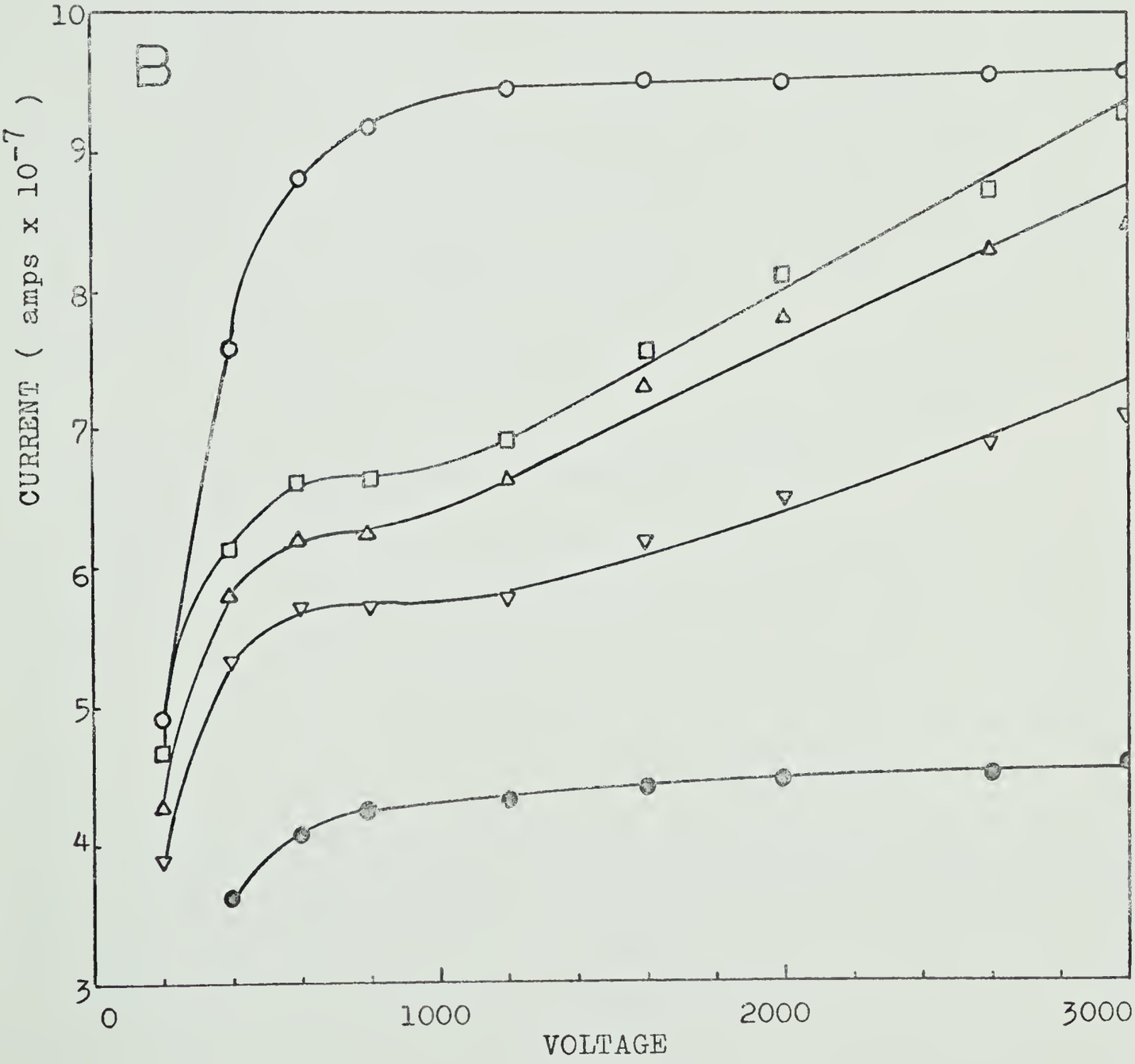
B
10
9
8
7
6
5
4
3
0
1000
2000
3000
VOLTAGE
CURRENT (amps x 10^{-7})

FIGURE III - 8

Decrease in Saturation Currents with Temperature at Different Pressures When Side of Pyrex Cell with Aluminium Electrodes Painted with Aquadag and Grounded

Net Positive and Negative Currents

A. Hydrogen : Pressure at 25.2°C = 50 torr
Density = 5.37×10^{-6} gm/cm^3

B. Hydrogen : Pressure at 26.0°C = 307 torr
Density = 3.19×10^{-5} gm/cm^3

C. Air : Pressure at 25.0°C = 53 torr
Density = 8.26×10^{-5} gm/cm^3

D. Air : Pressure at 25.2°C = 300 torr
Density = 4.64×10^{-4} gm/cm^3

○ : + ve current at 25°C

● : - ve current at 25°C

□ : + ve current at 110°C

■ : - ve current at 110°C

△ : + ve current at 170°C

▲ : - ve current at 170°C

Background Currents

The following background currents were measured.

25°C : $\simeq 10^{-10}$ amps at ± 3000 V

110°C : $\simeq 10^{-10}$ amps at ± 3000 V

170°C : $\simeq 10^{-9}$ amps at ± 3000 V

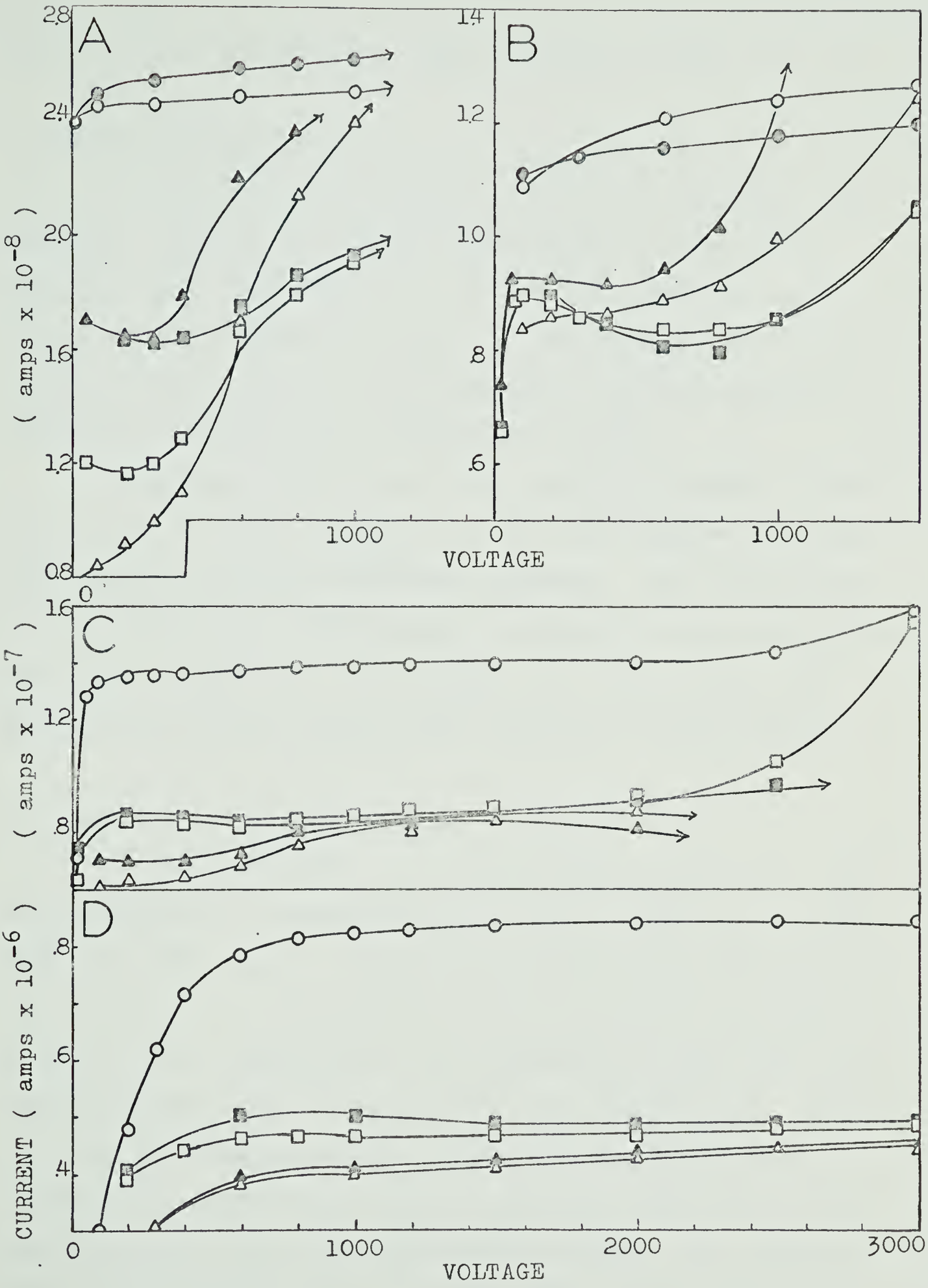
A
B
C
D
2.8
2.4
2.0
1.6
1.2
0.8
1.4
1.2
1.0
.8
.6
1.6
1.2
.8
.8
.6
.4
(amps x 10⁻⁸)
(amps x 10⁻⁷)
CURRENT (amps x 10⁻⁶)
1000
0
1000
0
1000
2000
3000
VOLTAGE
VOLTAGE

uration current increased. This is shown in Fig. III - 9.

G. Pyrex Spherical Cell

The current collected at the outer electrode was measured. Saturation current measurements in the Pyrex spherical cell (see Fig. II - 2A) for air, hydrogen, and helium showed a gradual increase in the plateaus with temperature, even with the outer surface of the cell grounded. Background currents began appearing at 140°C.

For all three gases, the positive currents reached saturation at lower voltages than did the negative currents, and also gave greater saturation plateaus. The differences in the positive and negative net currents for air and helium are shown in Fig. III - 10 and III - 11. The effect with hydrogen was midway between that found for air and helium.

H. Conductance of a Pyrex Plug

The conductance of a Pyrex plug (see Fig. II - B) was determined at temperatures from 25° to 200°C at 0, 1000, 2000, and 3000 volts. The plug was washed with 95% alcohol, and the positive and negative currents that were obtained at the various temperatures are tabulated in Table III - 3. These currents were not very steady nor reproducible. There was a slight difference in current readings depending on whether the sample heater power supply was turned off or on during the time that the readings were taken. All measurements recorded were taken with the power supply turned off.

FIGURE III - 9

Percent Decrease in Saturation Current for Different Ratios of Diameter (d) of Electrodes to Distance (l) Between Electrodes

Air: Pressure at 25°C = 300 torr

Density = 0.468×10^{-3} gm/cm^3

○ : 110°C

● : 170°C

Hydrogen: Pressure at 25°C = 300 torr

Density = 0.325×10^{-4} gm/cm^3

■ : 170°C

Helium: Pressure at 25°C = 300 torr

Density = 0.645×10^{-4} gm/cm^3

△ : 110°C

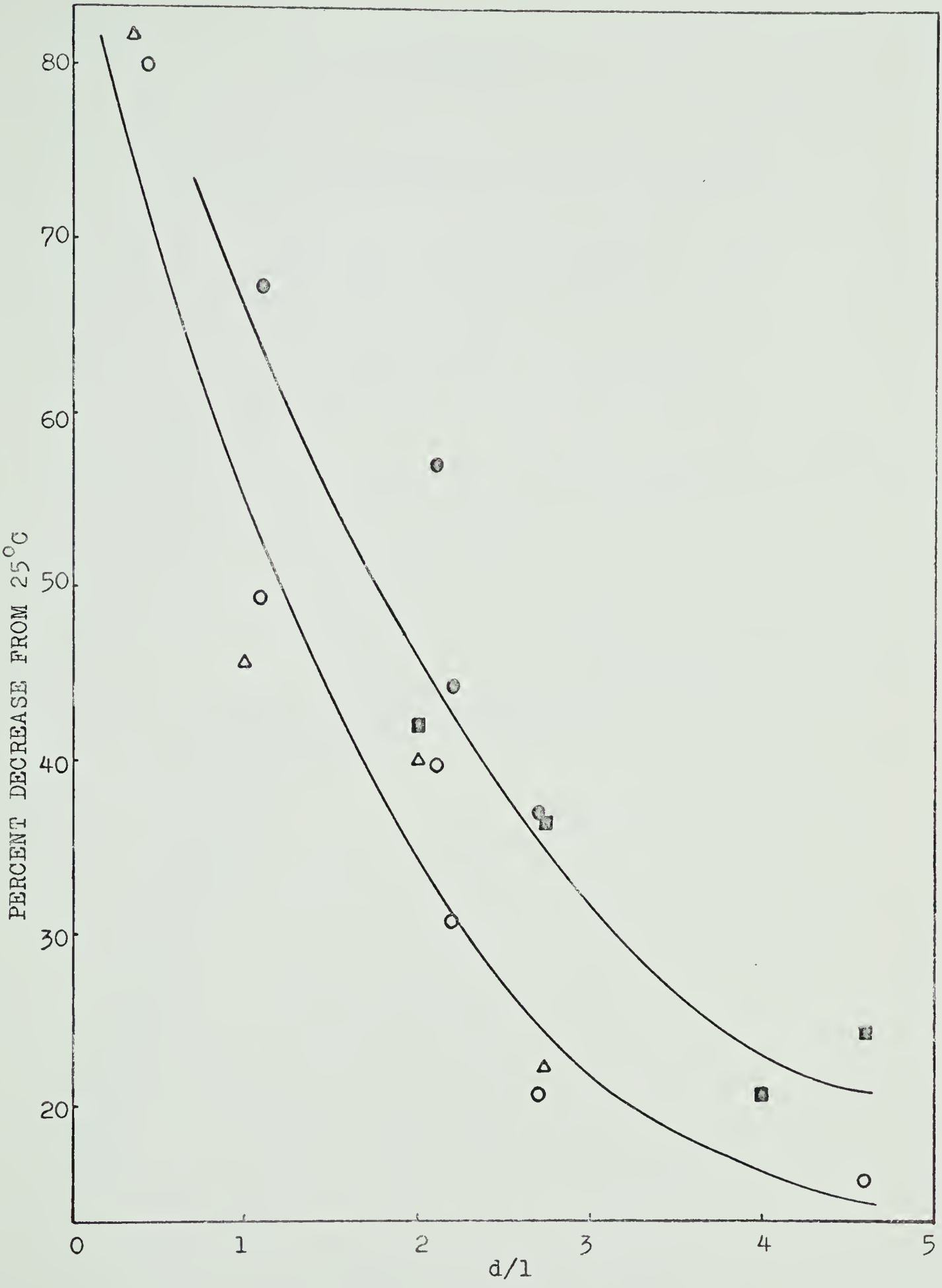
80
70
60
50
40
30
20
PERCENT DECREASE FROM 25°C
0
1
2
3
4
5
d/l

FIGURE III - 10

Currents Measured in Pyrex Spherical Cell

Air : Pressure at 25°C = 150 torr

Density = 0.234×10^{-3} gm/cm^3

A. Background Currents

□ : positive current at 110°C

■ : negative current at 110°C

▽ : positive current at 170°C

▼ : negative current at 170°C

In addition, the following background currents were measured.

25°C : $\simeq 10^{-10}$ amps at $\pm$ 3000 V

B. Net Currents

○ : positive current at 25°C

● : negative current at 25°C

□ : positive current at 110°C

■ : negative current at 110°C

▽ : positive current at 170°C

▼ : negative current at 170°C

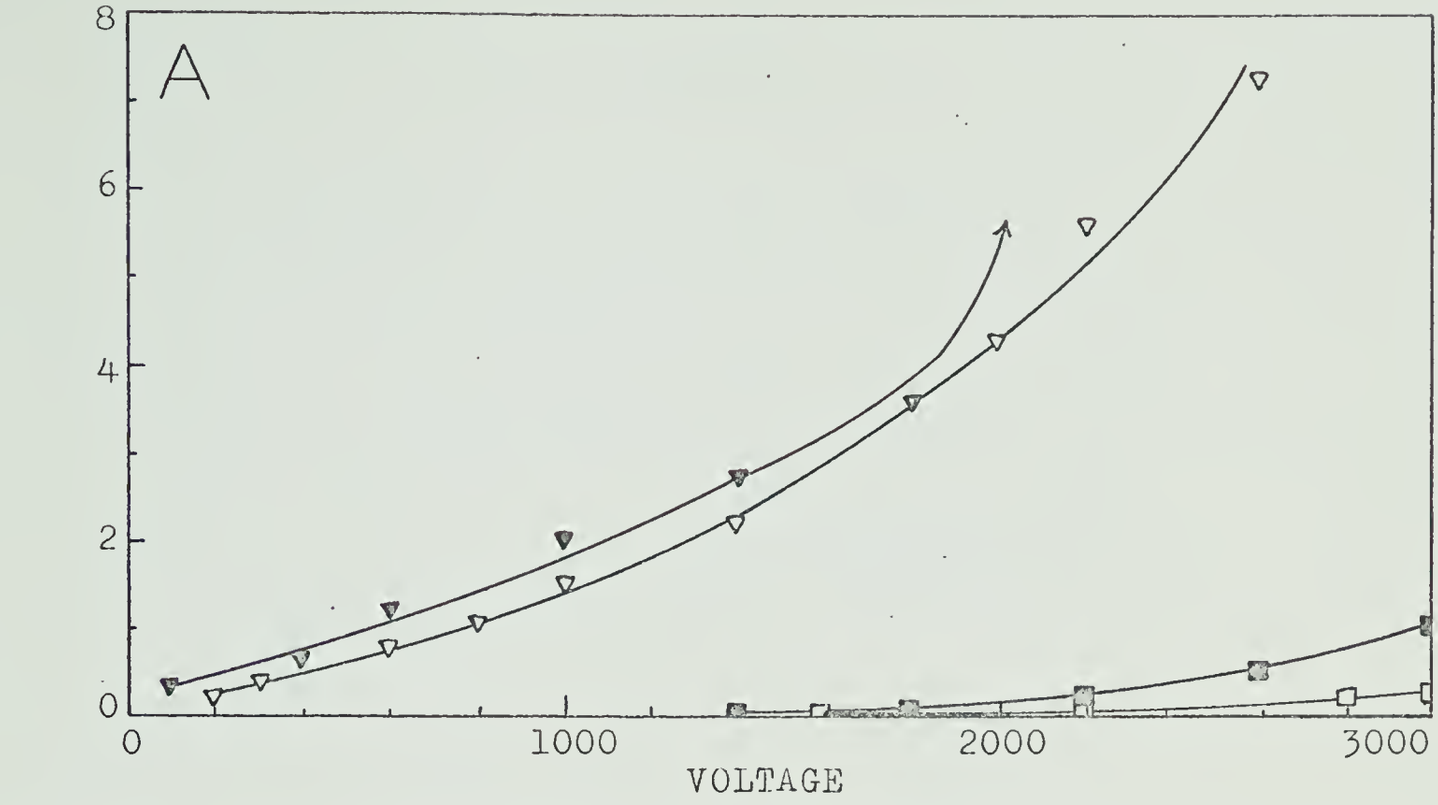
A
8
6
4
2
0
0
1000
2000
3000
VOLTAGE

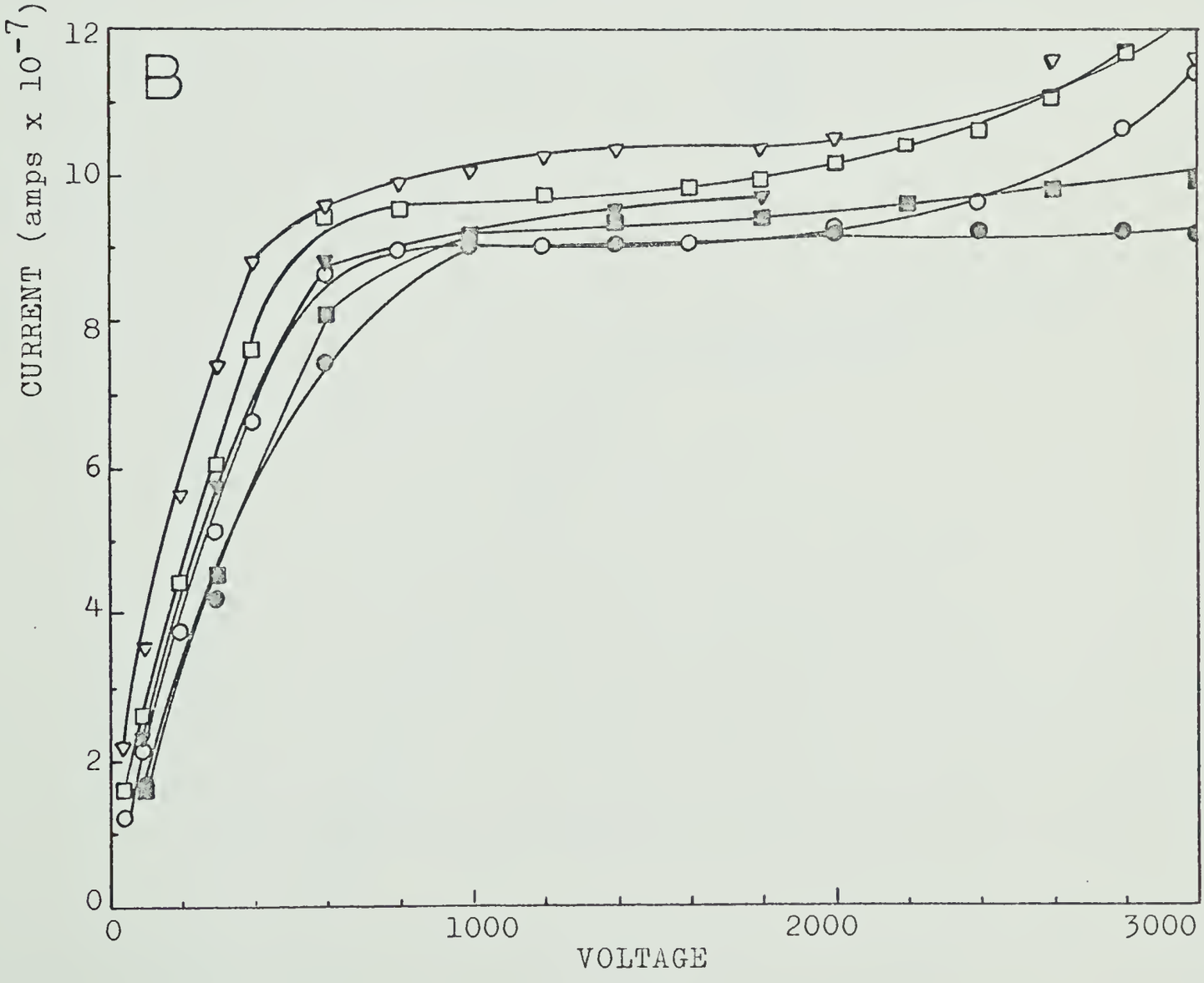
B
CURRENT (amps x 10^{-7})
12
10
8
6
4
2
0
0
1000
2000
3000
VOLTAGE

FIGURE III - 11

Currents Measured in Pyrex Spherical Cell

Helium : Pressure at 25°C = 295 torr

Density = 2.34×10^{-4} gm/cm^3

A. Background Currents

▽ : positive current at 170°C

▼ : negative current at 170°C

In addition, the following background currents were measured.

25°C : $\simeq 10^{-10}$ amps at ± 500 V

80°C : $\simeq 10^{-9}$ amps at ± 500 V

110°C : $\simeq 3.9 \times 10^{-9}$ amps at ± 500 V

B. Net Currents

○ : positive current at 25°C

● : negative current at 25°C

□ : positive current at 80°C

■ : negative current at 80°C

△ : positive current at 110°C

▲ : negative current at 110°C

▽ : positive current at 170°C

▼ : negative current at 170°C

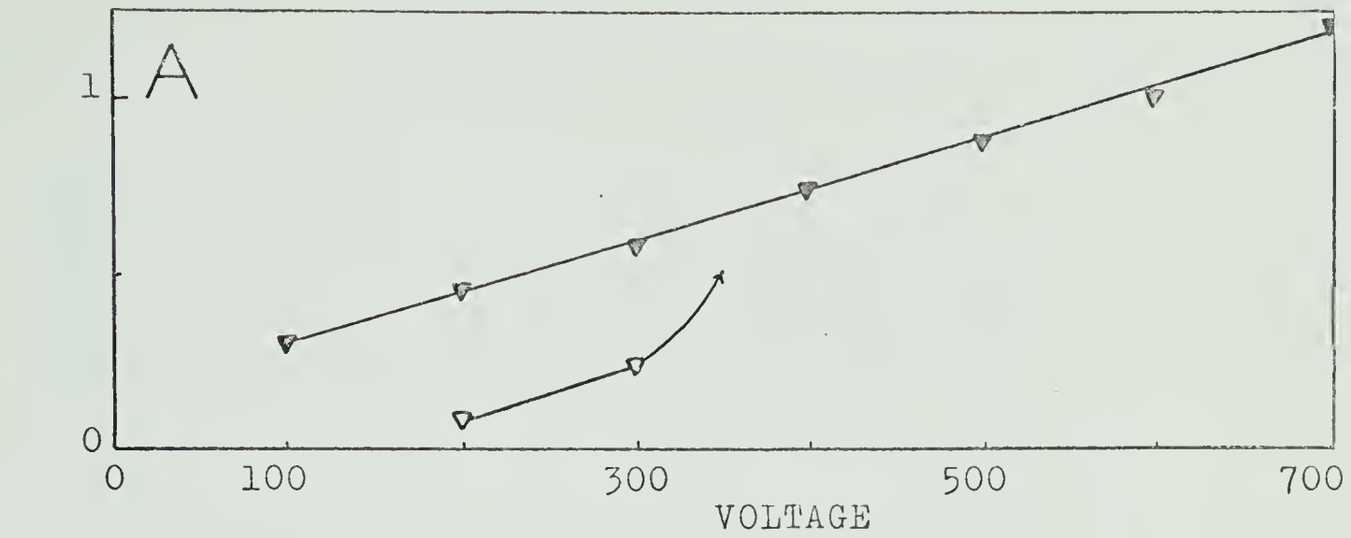
A
1
0
0
100
300
500
700
VOLTAGE

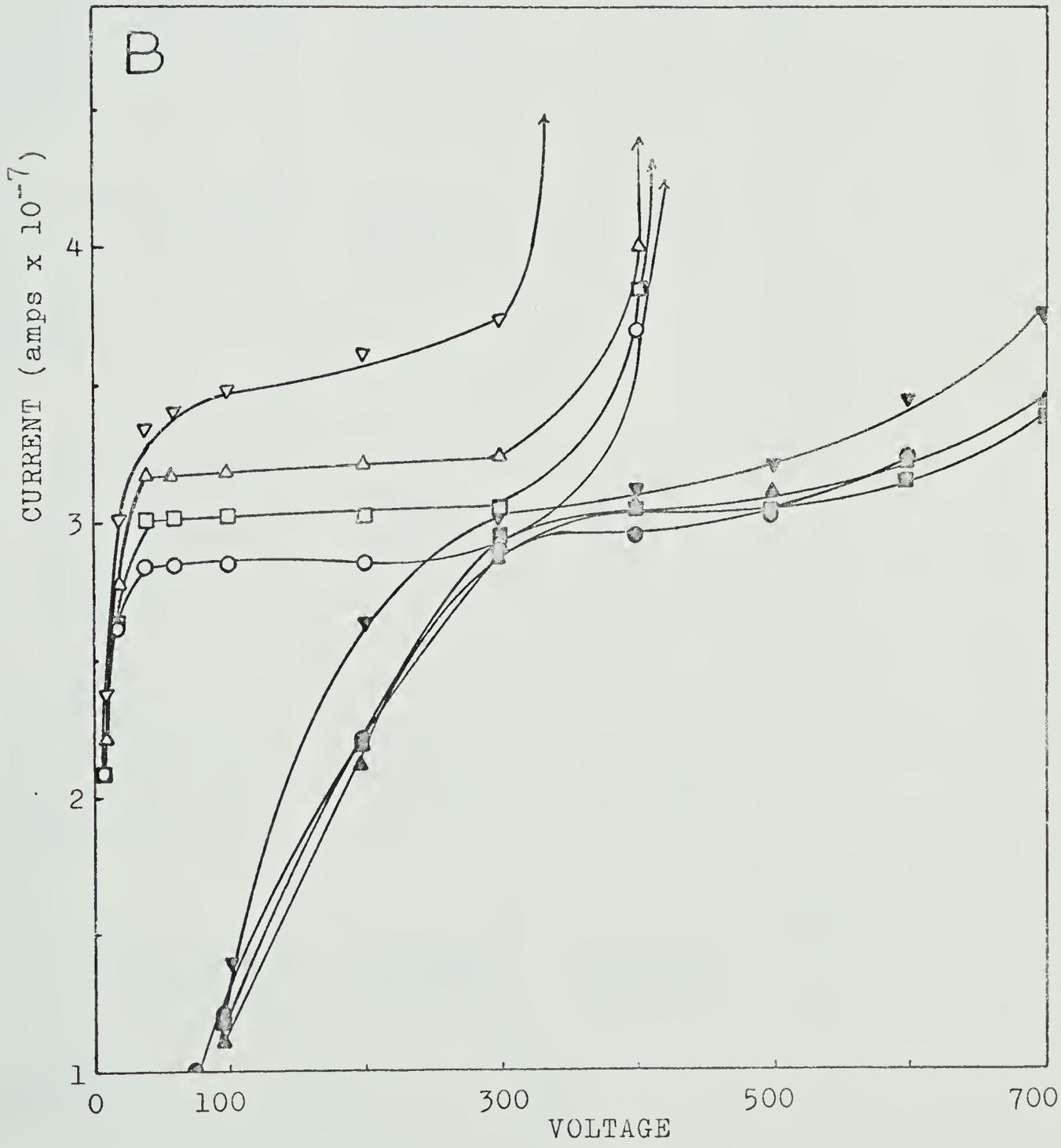
B
CURRENT (amps x 10^{-7})
4
3
2
1
0
100
300
500
700
VOLTAGE

TABLE III-3

Conductance of a Pyrex Plug*

Plug Under Irradiation**				Plug Not Irradiated			
Temp (°C)	Volts	Current at +ve Voltage	Current at -ve Voltage	Temp (°C)	Volts	Current at +ve Voltage	Current at -ve Voltage
25	0	-2.4×10^{-10}		25	0	$+1.5\times10^{-12}$	
	1000	-1.4×10^{-10}	-3.1×10^{-10}		1000	$+9.5\times10^{-12}$	$+1.0\times10^{-12}$
	2000	-7.5×10^{-11}	-3.5×10^{-10}		2000	$+1.3\times10^{-11}$	-5.2×10^{-12}
	3000	$+6.0\times10^{-11}$	-4.2×10^{-10}		3000	$+1.5\times10^{-11}$	-1.0×10^{-11}
110	0	$+9.0\times10^{-10}$		110	0	$+3.0\times10^{-11}$	
	1000	$+6.2\times10^{-9}$	-4.5×10^{-9}		1000	$+1.1\times10^{-8}$	-1.2×10^{-8}
	2000	$+1.3\times10^{-8}$	-1.0×10^{-8}		2000	$+2.2\times10^{-8}$	-2.4×10^{-8}
	3000	$+2.1\times10^{-8}$	-1.7×10^{-8}		3000	$+8.9\times10^{-8}$	-3.2×10^{-8}
170	0	$+4.1\times10^{-9}$		170	0	-1.6×10^{-10}	
	1000	$+5.4\times10^{-7}$	-6.0×10^{-7}		1000	$+7.3\times10^{-7}$	-7.9×10^{-7}
	2000	$+1.2\times10^{-6}$	-1.3×10^{-6}		2000	$+1.4\times10^{-6}$	-1.6×10^{-6}
	3000	$+1.9\times10^{-6}$	-2.0×10^{-6}		3000	$+2.2\times10^{-6}$	-2.4×10^{-6}

* The distance between the tungsten electrodes in the Pyrex was 3 mm.

** Absorbed dose rate = 7.1×10^{19} eV/g hr.

TABLE III-4

Conductance of a Pyrex Plug Wrapped With Teflon Tape*

Plug Under Irradiation**				Plug Not Irradiated			
Temp (°C)	Volts	Current at +ve Voltage	Current at -ve Voltage	Temp (°C)	Volts	Current at +ve Voltage	Current at -ve Voltage
25	0	-3.3×10^{-10}		25	0	-9.0×10^{-13}	
	1000	-7.4×10^{-11}	-5.7×10^{-10}		1000	$+2.5\times10^{-12}$	-6.0×10^{-12}
	2000	$+1.6\times10^{-10}$	-7.5×10^{-10}		2000	$+6.0\times10^{-12}$	-7.0×10^{-12}
	3000	$+4.2\times10^{-10}$	-9.5×10^{-10}		3000	$+1.0\times10^{-11}$	-1.0×10^{-11}
110	0	$+1.5\times10^{-9}$		110	0	$+9.0\times10^{-12}$	
	1000	$+3.2\times10^{-8}$	-3.1×10^{-8}		1000	$+1.2\times10^{-8}$	-1.7×10^{-8}
	2000	$+6.0\times10^{-8}$	-6.2×10^{-8}		2000	$+2.7\times10^{-8}$	-3.1×10^{-8}
	3000	$+9.2\times10^{-8}$	-9.4×10^{-8}		3000	$+3.8\times10^{-8}$	-5.0×10^{-8}
170	0	$+5.0\times10^{-9}$		170	0	$+3.4\times10^{-10}$	
	1000	$+1.7\times10^{-7}$	-1.5×10^{-6}		1000	$+1.2\times10^{-6}$	-1.3×10^{-6}
	2000	$+3.5\times10^{-6}$	-3.2×10^{-6}		2000	$+2.5\times10^{-6}$	-2.8×10^{-6}
	3000	$+5.6\times10^{-6}$	-5.0×10^{-6}		3000	$+3.9\times10^{-6}$	-4.4×10^{-6}

* The distance between the tungsten electrodes in the Pyrex was 3 mm.

** Absorbed dose rate = 7.1×10^{19} eV/g hr.

I. Effect of Wrapping Outer Surface of Cell and of Plug with Teflon Tape

When the Pyrex plug and leads were wrapped completely with teflon tape, the conductance at the higher temperatures was almost the same in the presence and absence of the radiation field. The positive and negative currents that were obtained at the different temperatures are given in Table III - 4.

The Pyrex parallel-plate cell (Figure II - 1A) with aluminium electrodes was filled, as previously, with 300 torr of hydrogen. The outside of the cell was washed with 95% alcohol and wrapped with teflon tape. Positive and negative saturation current measurements were taken at 25°C and 170°C. The net currents obtained at 170°C were lowered by only 14% as compared to 410% without the teflon wrapping. In the latter case, the net current was actually negative.

The Pyrex spherical cell was filled with 302 torr of helium, the outside of the cell was washed with 95% alcohol and wrapped with teflon tape. The increase in the positive saturation current was only about 2% as compared to 33% when the cell was not wrapped with teflon tape. The negative saturation currents gave an increase of 13% in the wrapped cell, compared to 6% in the unwrapped cell. In both cells there was a discharge in the positive saturation currents at approximately the same voltage at which the negative current reached saturation. These currents in the wrapped cell are illustrated in Figure III - 12 and those

FIGURE III - 12

Currents Measured in Pyrex Spherical Cell Wrapped With Teflon Tape

Helium : Pressure at 25°C = 302 torr

Density = 6.53×10^{-5} gm/cm^3

A. Background Currents

▽ : positive current at 170°C

▼ : negative current at 170°C

In addition, the following background currents were measured.

25°C : $+ 1.0 \times 10^{-11}$ amps at + 800 V

$- 0.5 \times 10^{-11}$ amps at - 800 V

B. Net Currents

○ : positive current at 25°C

● : negative current at 25°C

▽ : positive current at 170°C

▼ : negative current at 170°C

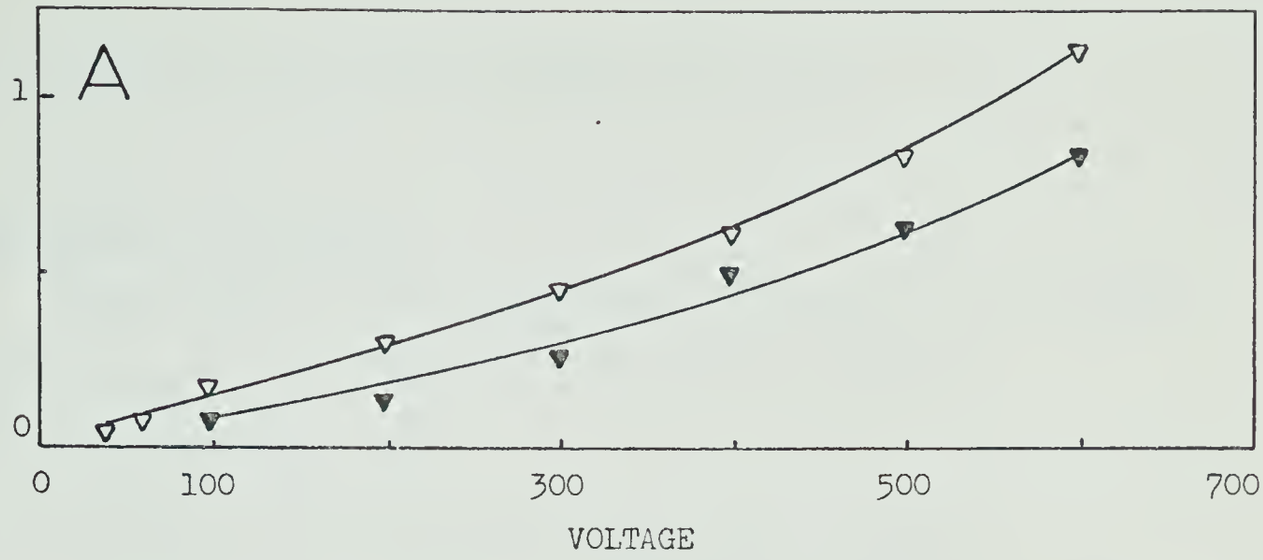
A
1
0
0
100
300
500
700
VOLTAGE

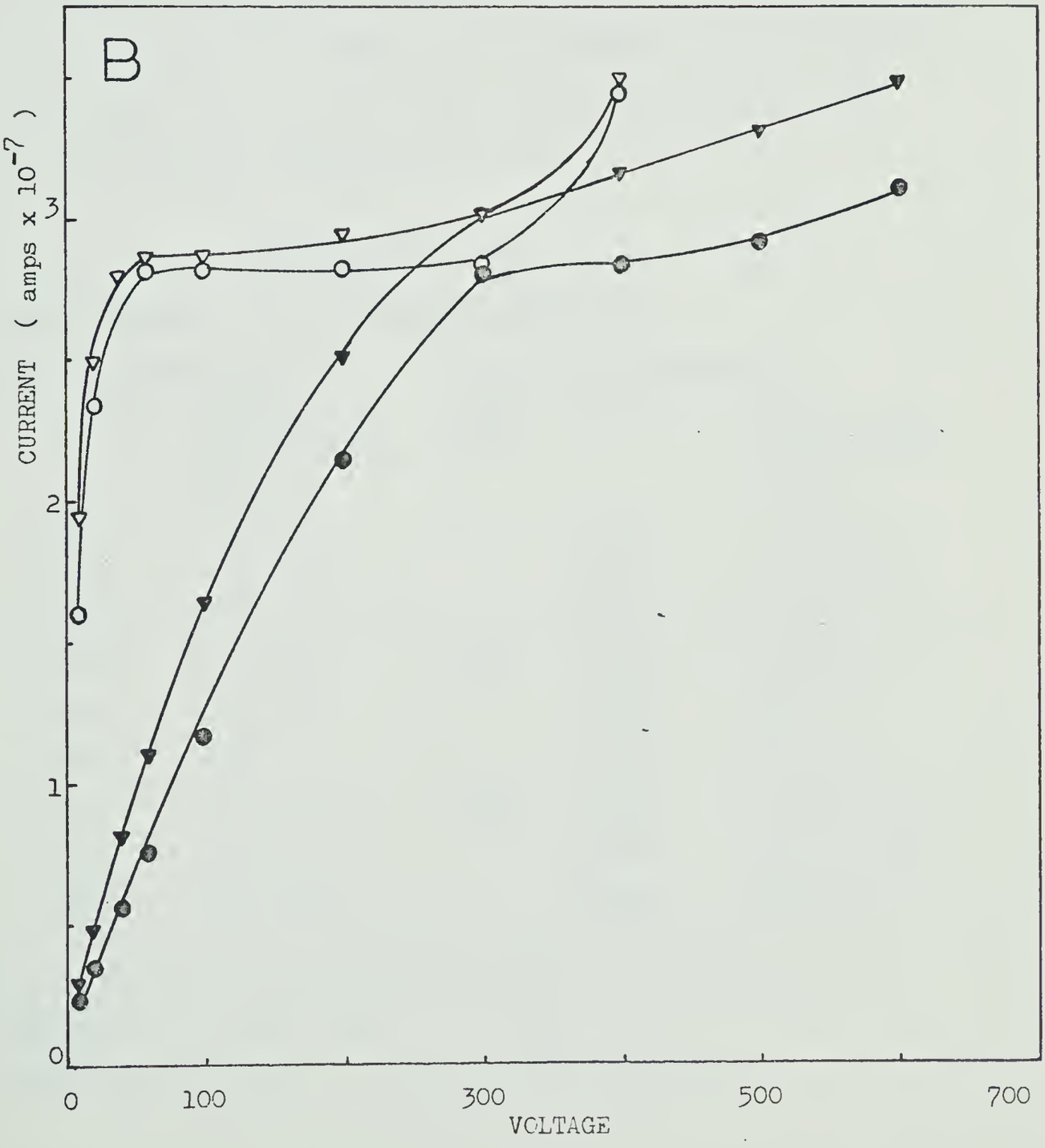
B
CURRENT (amps x 10⁻⁷)
3
2
1
0
0
100
300
500
700
VOLTAGE

in the unwrapped cells are in Figure III - 11.

2. CONDUCTANCE OF CERAMIC

Conductance plugs, similiar in design to the Pyrex plug, were constructed from the following ceramics:

i . Supramica 500

ii. 502-400 Aremcolox Machinable Ceramics

iii. 505-600 Aremcolox Machinable Ceramics

The positive conductance currents of the three different types of ceramics were nearly the same. The results are given in Table III - 4a.

TABLE III - 4a

Conductance of a Supramica 500 Plug*

Plug Under Irradiation**			Plug Not Irradiated		
Temp. (°C)	Volts	Current at +ve Voltage (Amps)	Temp. (°C)	Volts	Current at +ve Voltage (Amps)
25	1000	3.2×10^{-9}	25	1000	2.3×10^{-12}
	2000	5.7×10^{-9}		2000	5.4×10^{-12}
	3000	8.2×10^{-9}		3000	9.4×10^{-12}
110	1000	1.7×10^{-9}	110	1000	9.3×10^{-12}
	2000	8.4×10^{-9}		2000	10×10^{-11}
	3000	10×10^{-9}		3000	2.3×10^{-11}
170	1000	7.5×10^{-9}	170	1000	6.7×10^{-11}
	2000	11.0×10^{-9}		2000	15.0×10^{-11}
	3000	13.4×10^{-9}		3000	27.0×10^{-11}

* The distance between the tungsten electrodes in the Supramica 500 was 3 mm.

** Absorbed dose rate 3.0×10^{19} eV/g hr.

The ceramics had a lower conductance than did Pyrex, but unfortunately it was not possible to obtain a vacuum tight ceramic that would withstand the temperature changes of the present experiments.

3. QUARTZ CELL

A. Conductance of Quartz

The conductivity of a Quartz plug was determined in the presence and absence of radiation. The conductivity of the quartz plug at 110°C and 170°C was smaller than the conductivity of the ceramics and Pyrex plugs by factors of 10 and 10,000 respectively. The values of the positive and negative currents obtained at the various temperatures and voltages are presented in Table III - 5.

B. Temperature Effect in a Quartz Cell with Parallel-plate Electrodes

When saturation current measurements were taken in the Quartz cell (stainless steel electrodes which did not touch the walls) only a small percent decrease in the saturation currents at the different temperatures were observed. With an initial pressure of 302 torr of air at 27.4°C, there was only an approximate 2% decrease in the positive and negative saturation currents at 170°C from the saturation currents at 25°C.

TABLE III-5

Conductance of a Quartz Plug*

Plug Under Irradiation**				Plug Not Irradiated			
Temp (°C)	Volts	Current at +ve Voltage	Current at -ve Voltage	Temp (°C)	Volts	Current at +ve Voltage	Current at -ve Voltage
25	0	-1.80×10^{-10}		25	0	$+1.1\times10^{-12}$	
	1000	-1.56×10^{-10}	-2.01×10^{-10}		1000	$+1.3\times10^{-12}$	$+0.55\times10^{-12}$
	2000	-1.37×10^{-10}	-2.14×10^{-10}		2000	$+1.3\times10^{-12}$	$+0.45\times10^{-12}$
	3000	-1.14×10^{-10}	-2.30×10^{-10}		3000	$+1.4\times10^{-12}$	$+0.30\times10^{-12}$
110	0	-0.2×10^{-9}		110	0	----------	
	1000	-1.7×10^{-10}	-0.3×10^{-9}		1000	Unsteady currents in the	
	2000	$+2.0\times10^{-10}$	-0.45×10^{-9}		2000	vicinity of 10^{-11}. Unable	
	3000	Unsteady-10^{-10}	-0.64×10^{-9}		3000	to take meaningful readings.	
170	0	-0.1×10^{-9}		170	0	----------	
	1000	-0.1×10^{-9}	-0.6×10^{-9}		1000	Unsteady currents in the	
	2000	$+0.1\times10^{-9}$	-0.6×10^{-9}		2000	vicinity of 10^{-11}. Unable	
	3000	$+0.5\times10^{-9}$	-1.0×10^{-9}		3000	to take meaningful readings.	

* The distance between the tungsten electrodes in the Quartz was 2.5 mm.

**Absorbed dose rate = 3.0×10^{19} eV/g hr.

Saturation current measurements were taken in the same Quartz cell filled with 298 torr of hydrogen at 28.4°C. Positive and negative current measurements were taken at the different temperatures. While the current readings were being recorded, the sample heater power supply was turned off. The saturation current measurements that were observed at 25, 80, 110, 140, and 170°C were the same. When the power supply was turned off there was only a slight difference from the current that was observed when the power supply was on.

4. STEEL SPHERICAL CELL

Positive and negative saturation current measurements were taken in the stainless steel spherical cell (see Fig. II - 3B) at three different temperatures. The cell was filled with 301 torr of air at 24.8°C. Current readings were recorded when the sample heater power supply was turned off. The voltages required to reach negative saturation currents were greater than the voltages required to reach positive saturation currents. The positive and negative saturation currents were the same size, and there was no variation in the saturation current with temperature. The saturation currents obtained are shown in Fig. III - 13.

5. DOSE RATE EFFECT

In order to study the effect of dose rate on the net saturation currents at different temperatures, current

FIGURE III - 13

Saturation Currents in Stainless Steel Spherical Cell

Hydrogen : Pressure at 24.8°C = 30.1 cm

Density = 0.0329×10^{-3} gm/cc

Net Positive and Negative Currents

25°C	○	: + ve current	●	:	- ve current
110°C	□	: + ve current	■	:	- ve current
170°C	△	: + ve current	▲	:	- ve current

Background Currents

The following background currents were measured.

25°C : ± 2000 volts = $\pm 0.25 \times 10^{-10}$ amps

110°C : ± 2000 volts = $\pm 0.50 \times 10^{-8}$ amps

170°C : ± 1200 volts = $\pm 0.45 \times 10^{-7}$ amps

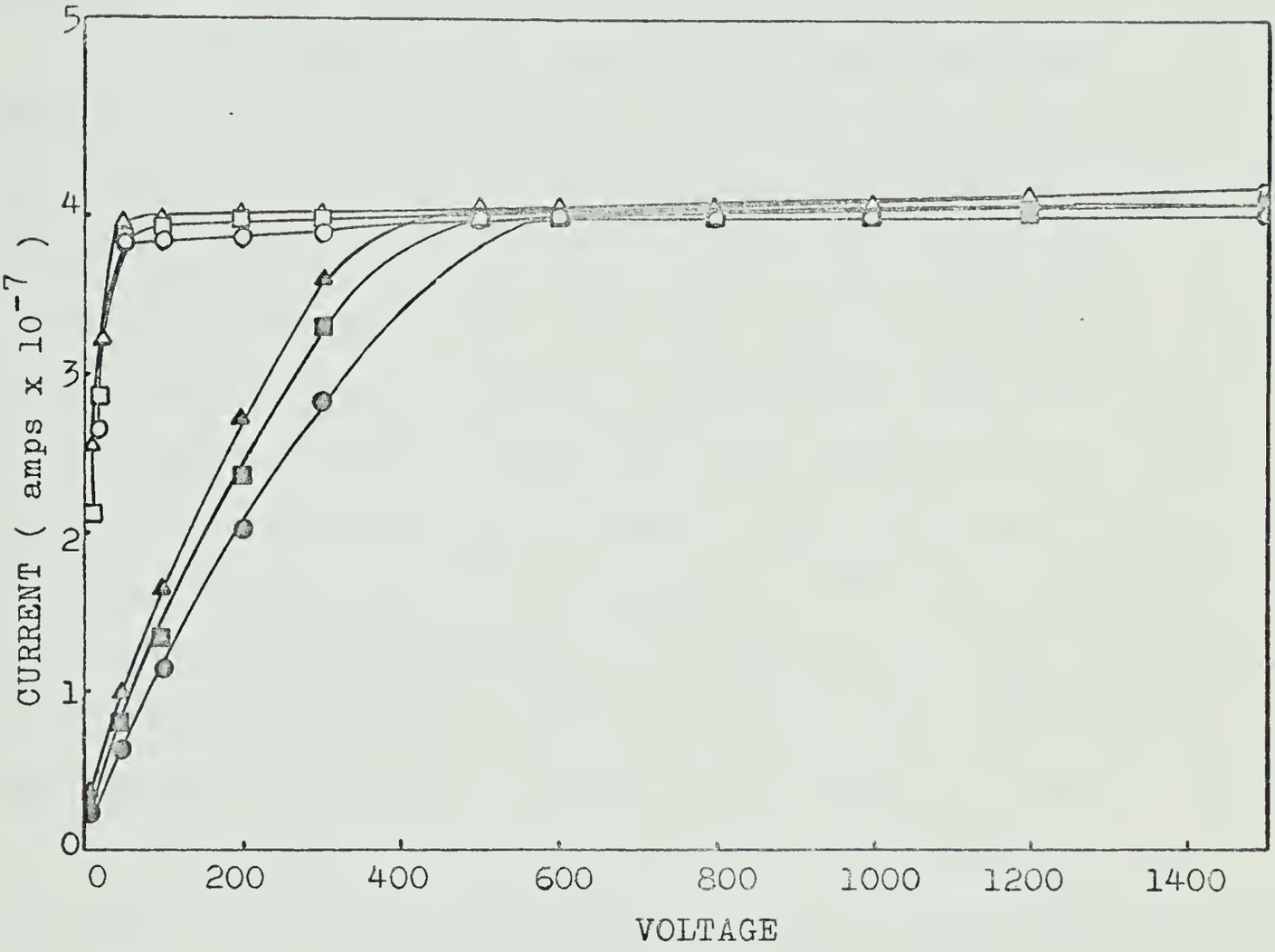
CURRENT (amps x 10^{-7})
0
1
2
3
4
5
0
200
400
600
800
1000
1200
1400
VOLTAGE

measurements in the Pyrex and Quartz cells containing air or hydrogen were taken in the irradiation cave. A variation of dose rate was obtained by positioning the cells at different distances from a 5000 curie cobalt-60 source. A summary of the results is shown in Table III-6.

The study of dose rate in the Pyrex cell containing hydrogen showed that when the dose rate was decreased by a factor of 6.7, the percent decrease at 110°C from the 25°C value of the net saturation current was independent of the dose rate (see Fig. III - 14). At both dose rates, the positive currents decreased slightly more than the negative currents. When the same cell was filled with air, and the dose rate decreased by a factor of 87, the percent decrease in the net saturation current at 110°C from the 25°C value at 1000 volts decreased by a factor of 1.3 (Fig. III-15, D, E). The positive and negative currents were almost the same. Thus, the effect of dose rate is relatively small.

The effect of dose rate on the net saturation currents was investigated over a wider range of temperature in the Quartz cell than in the Pyrex cell because the temperature effect in Quartz was even smaller than in Pyrex. The dose rate effect with temperature was negligible when the quartz cell contained hydrogen, and the percent decrease from the 25°C value was only 9% of that in the Pyrex cell. When the Quartz cell was filled with air and the dose rate decreased by factors of 8.8 and 102, the decreases in the net

saturation currents between 25° and 170°C, taken at 1000 volts, were about zero, 9% and 15% respectively (Fig. III - 15, A, B, C). Again, there was little difference in the negative and positive saturation currents.

TABLE III - 6

Dose Rate Effect on Net Saturation Current

Cell	Dose Rate (eV/cm^3 sec)	Temp (^oC)	Saturation Current (amps) at 1000 V	Decrease from 25°C at 1000 V	Per Cent Decrease at 1000 V
Hydrogen: 3.1×10^{-5} gm/cm^3					
Pyrex	8.1×10^{10}	25	1.54×10^{-8}		
		110	$+8.0 \times 10^{-9}$	7.4×10^{-9}	48.1
		110	-9.6×10^{-9}	5.8×10^{-9}	37.7
Pyrex	8.1×10^{11}	25	1.54×10^{-7}		
		110	$+7.6 \times 10^{-8}$	7.8×10^{-8}	50.6
		110	-8.8×10^{-8}	6.6×10^{-8}	42.9
Hydrogen: 3.0×10^{-5} gm/cm^3					
Quartz	1.0×10^{11}	25	2.13×10^{-8}		
		170	2.03×10^{-8}	0.1×10^{-8}	4.8
Quartz	9.6×10^{11}	25	1.97×10^{-7}		
		170	1.90×10^{-7}	0.07×10^{-7}	3.6
Air: 4.5×10^{-4} gm/cm^3					
Pyrex	5.4×10^{10}	25	1.00×10^{-8}		
		110	6.60×10^{-9}	3.4×10^{-9}	34
Pyrex	6.2×10^{12}	25	1.16×10^{-6}		
		110	9.00×10^{-7}	2.6×10^{-7}	22.4
Air: 4.7×10^{-4} gm/cm^3					
Quartz	4.4×10^{10}	25	9.4×10^{-9}		
		170	8.0×10^{-9}	1.4×10^{-9}	14.9
Quartz	5.0×10^{11}	25	1.1×10^{-7}		
		170	1.0×10^{-7}	0.1×10^{-7}	9.1
Quartz	4.3×10^{12}	25	9.1×10^{-7}		
		170	9.1×10^{-7}	0.0×10^{-7}	0

FIGURE III - 14

Dose Rate Effect in Pyrex Cell With Aluminium Electrodes

Hydrogen : Pressure at 26.2°C = 300 torr

Density = 3.1×10^{-5} gm/cm^3

Dose Rate

B : 8.1×10^{10} eV/cm^3 sec

C : 8.1×10^{11} eV/cm^3 sec

Background Currents of B and C

□ : +ve current at 110°C

■ : -ve current at 110°C

In addition, the following background currents were measured.

25°C : 1.0×10^{-11} amps at + 3000 V

Net Currents

o : +ve current at 25°C

(-ve current $\simeq$ +ve current)

□ : +ve current at 110°C

■ : -ve current at 110°C

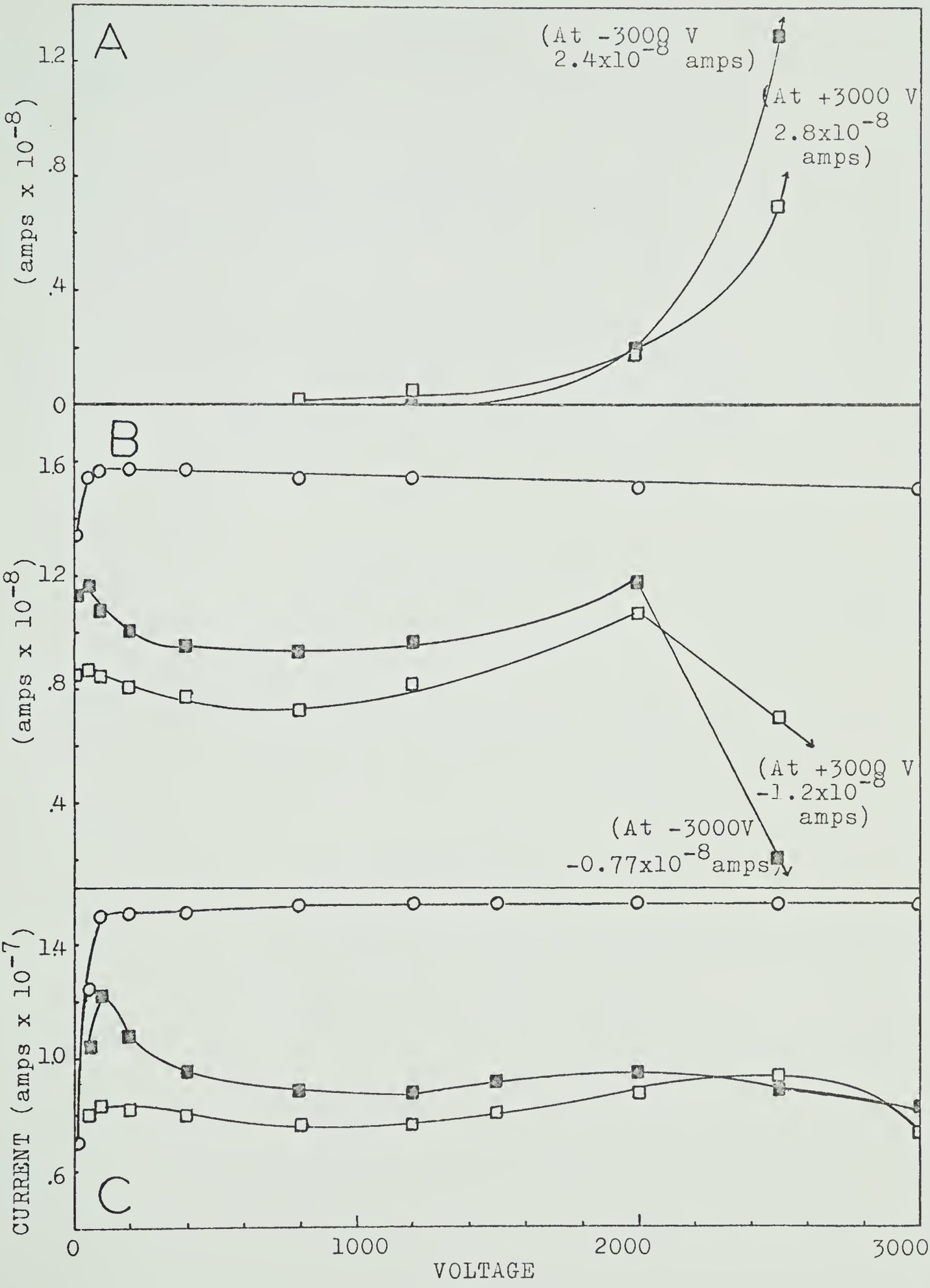
A
(At -3000 V
2.4x10^-8 amps)
(At +3000 V
2.8x10^-8
amps)
1.2
.8
.4
0
(amps x 10^-8)
B
1.6
1.2
.8
.4
(amps x 10^-8)
(At +3000 V
-1.2x10^-8
amps)
(At -3000V
-0.77x10^-8amps)
1.4
1.0
.6
CURRENT (amps x 10^-7)
C
0
1000
2000
3000
VOLTAGE

FIGURE III - 15

Dose Rate Effect in Quartz Cell With Stainless Steel Electrodes

Air: Pressure at 26.0°C = 300 torr
Density = 4.7×10^{-4} gm/cm^3

Dose Rate
A : 4.4×10^{10} eV/cm^3 sec
B : 5.0×10^{11} eV/cm^3 sec
C : 4.3×10^{12} eV/cm^3 sec

Background Currents of A, B, and C at
25°C - 10^{-12} amps at +3000 V
170°C- 10^{-9} amps at +3000 V

Net Currents
o : +ve current at 25°C
Δ : +ve current at 170°C
(-ve current ≙ +ve current)

Dose Rate Effect in Pyrex Cell With Aluminium Electrodes

Air: Pressure at 26.5°C = 304 torr
Density = 4.5×10^{-4} gm/cm^3

Dose Rate
D : 5.4×10^{10} eV/cm^3 sec
E : 6.2×10^{12} eV/cm^3 sec

Background Currents of D and E at
+3000V, 25°C - 10^{-10} amps
+3000V, 110°C - 10^{-9} amps

Net Currents
o : +ve current at 25°C
□ : +ve current at 110°C
(-ve current ≙ +ve current)

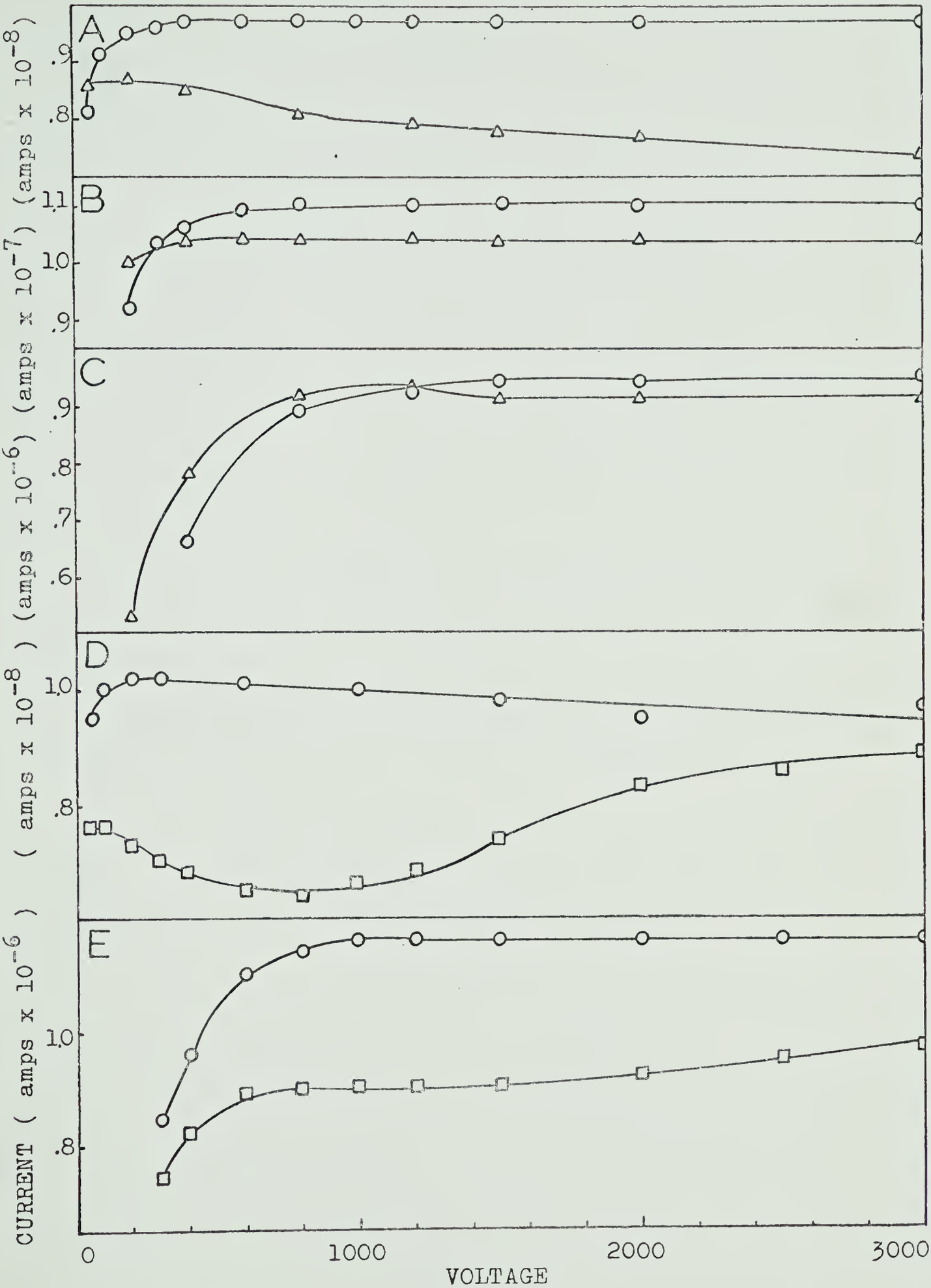
A
B
C
D
E
.9
.8
1.1
1.0
.9
.9
.8
.7
.6
1.0
.8
1.0
.8
CURRENT (amps x 10^{-6}) (amps x 10^{-8}) (amps x 10^{-6}) (amps x 10^{-7}) (amps x 10^{-8})
0
1000
2000
3000
VOLTAGE

FIGURE III - 16

Dose Rate Effect in Quartz Cell With Stainless Steel Electrodes

Hydrogen : Pressure at 27.0°C = 302 torr

Density = 3.03×10^{-5} gm/cm^3

Dose Rate

A. 1.0×10^{11} ev/cm^3 sec

B. 9.6×10^{11} ev/cm^3 sec

Background Currents of A and B

25°C : Negligible

170°C : 4.1×10^{-10} amps at $\pm$ 3000 V

Net Currents

o : + ve current at 25°C

□ : + ve current at 170°C

(-ve current $\simeq$ +ve current)

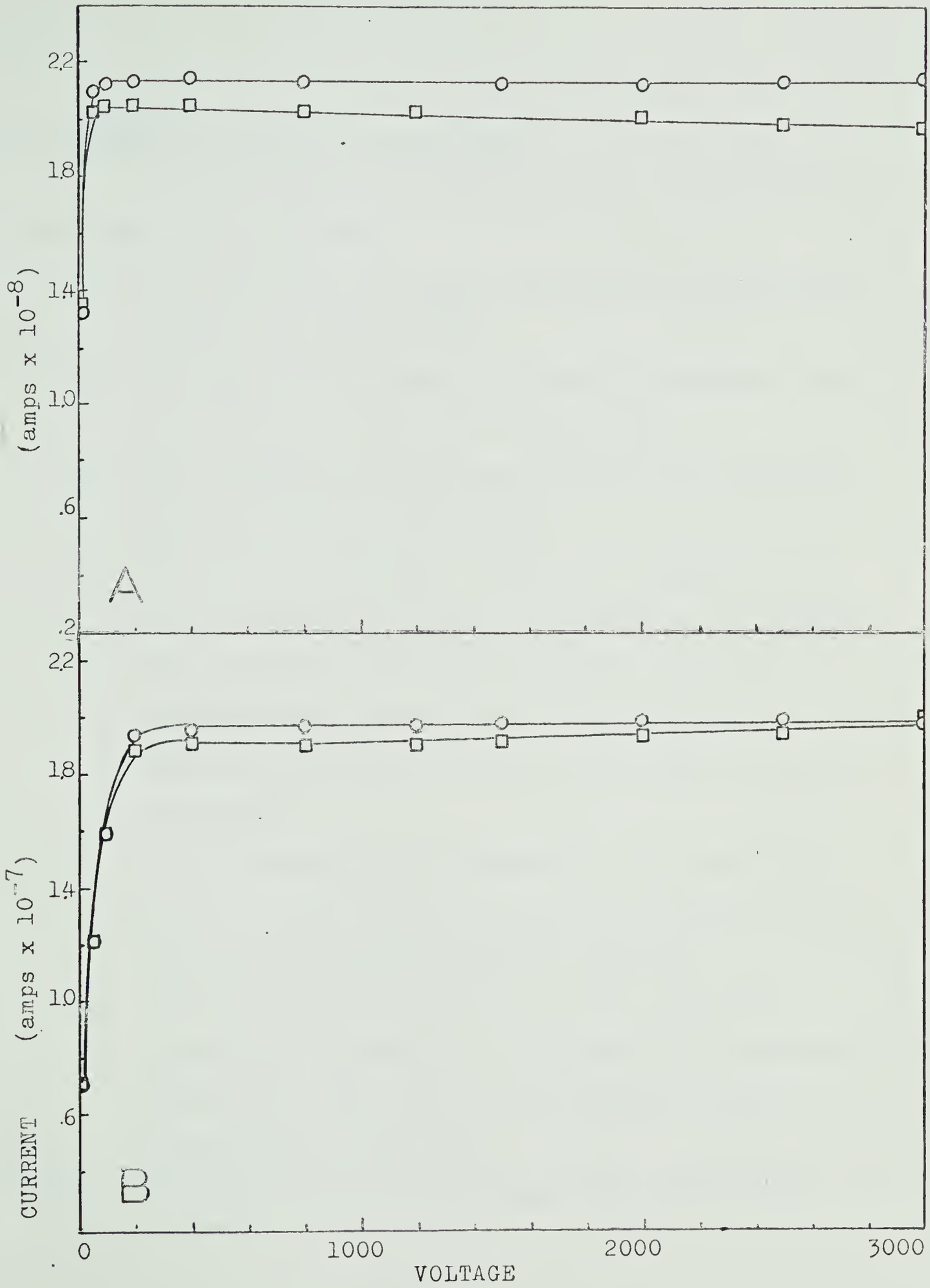
2.2
1.8
1.4
1.0
.6
.2
(amps x 10^{-8})
A
2.2
1.8
1.4
1.0
.6
CURRENT (amps x 10^{-7})
B
0
1000
2000
3000
VOLTAGE

D I S C U S S I O N

1. EFFECTS OBSERVED IN PYREX CELLS

The following is a summary of the observations which must be interpreted.

i. The saturation currents decreased at temperatures greater than about 50°C.

ii. The per cent decrease in saturation current from the 25° value varied from gas to gas.

iii. The background conductance of the cell increased with increasing temperature.

iv. The per cent decrease for the saturation current measurements for air were independent of pressure.

v. The saturation current was greater, but the per cent decrease was smaller, in the cell with platinium electrodes than in that with aluminium electrodes.

vi. Conditioning the cell decreased the temperature effect on the hydrogen saturation current but did not affect helium saturation currents.

vii. Painting the outer surface of the cell with aquadag and grounding it decreased the background current and also the current measured during irradiation of the cell.

viii. Saturation currents decreased with decreasing

value of the ratio of the diameter of the electrodes (d), to the distance between the electrodes (l).

ix. When the outer surface of the cell was wrapped with teflon tape, the temperature effect on the saturation current decreased.

x. The saturation currents were temperature dependent, regardless of whether the cell had spherical, cylindrical or parallel plate electrodes.

2. REASONS WHY THESE EFFECTS WERE UNEXPECTED

A. Temperature Coefficient of Ionization is Negligible

The ionization energy of atoms and molecules (about 10 eV) is so much larger than the thermal energies at the temperatures at which these experiments were performed that the temperature effect on ionization should be negligible in comparison to the effect of the 0.6 MeV Compton electrons. The difference (5) between these two effects can be illustrated by the following calculations:

(i) Effect on Ionization Due to the 0.6 MeV Compton Electrons

Consider the radiolysis of air at 0.5 atm pressure.

$$M \xrightarrow{I} M^+ + e^- ,$$

$$e^- + M^+ \xrightarrow{k_2} M^* ,$$

In the Gammacell-200 used in the present experiments, the rate of production of ions, I, in air at 0.5 atm pressure at

$300^{\circ}K$ is about 10^{11} ions/cc sec. At steady state:

$$\frac{d[M^+]}{dt} = 0 = I - k_2 [M^+][e^-] = I - k [M^+]^2$$

Since $[M^+] = [e^-]$

Therefore, $[M^+] = \left[\frac{I}{k}\right]^{1/2}$

The value of k_2 is about 10^{-6} cc/ion sec (9), so

$$[M^+] \simeq \left[10^{11} / 10^{-6}\right]^{1/2} \simeq 10^8 \text{ ions/cc.}$$

Thus the steady state concentration of ion pairs due to the 0.6 MeV Compton Electrons is about 10^8 ion pairs/cc.

(ii) Effect on Ionization Due to Thermal Energies

Consider the thermal production of ions in air at $300^{\circ}K$.

$$M \xrightarrow{k_1} M^+ + e^- \quad ,$$

$$M^+ + e^- \xrightarrow{k_2} M^* \quad ,$$

At steady state, since $[M^+] = [e^-]$,

$$\frac{d[M^+]}{dt} = 0 = k_1 [M] - k_2 [M^+]^2$$

and $$[M^+] = \left[(k_1 [M]) / k_2\right]^{1/2}$$

One may crudely estimate that

$$k_1 \simeq 10^{15} e^{-230000/RT}.$$

Then $10^{15}\ e^{-230000/(2x300)} = 10^{-152}$ cc/ion sec.

Since $k_2 \simeq 10^{-6}$ cc/ion sec (9) and $[M] \simeq 10^{19}$ molecules/cc

$$[M^+] \simeq \left[\left(10^{-152} x 10^{19}\right)/10^{-6}\right]^{\frac{1}{2}} = 10^{-64} \text{ ion/cc.}$$

Consequently, the number of ions produced by thermal energies is negligible in comparison to the number of ions produced by irradiation.

McClung has shown that the temperature coefficient of ionization for air, carbon dioxide, and hydrogen when subject to ionization to Roentgen rays is negligible between 14° and 200°C (6). This result was confirmed by Crowther (7) for air over a range of temperatures from -180° to +184°C, and for methyl iodide and ethyl bromide vapours from 25° to 184°C. Compton, Bennet, and Stearns (8) found an increase in ionization only at pressures over 100 atmospheres which was attributed to a decrease in initial recombination (to be discussed later) and not to an increase in energy absorption.

B. Recombination Coefficients Decrease as the Temperature Increases

A comparison of the temperature dependance of the recombination coefficients (k_2) with the mobilities of electrons and ions would indicate that the temperature should also have neglibible effect on ion collection at the voltages where saturation currents are obtained.

In the pressure region (50 to 300 torr at 25°C) and temperature range (25° - 170°C) used in the present work, ion recombination in the absence of an electric field is primarily homogeneous (9). Neutralization by homogeneous kinetics occurs when electrons escape recapture by parent ion, (initial recombination), and diffuse freely in the bulk medium. At 0.1 to 1 atmosphere pressure, the majority of the electrons travel more than 1μ from their parent ions before being thermalized. The mutual electric field between the ion and electron tends to draw them back together to recombine, whereas thermal kinetic energy, kt, tends to make the ion and electron move away from each other. The distance r at which the energy of coulombic attraction equals kt is given by the equation

$$r = e^2/\epsilon kt,$$

where ϵ is the dielectric constant of the medium and is essentially unity for gas at 1 atm pressure.

The probability (10) that the electron will escape from its parent ion is

$$e^{-r/y}$$

where y is the distance between the ion and the electron at the instance the electron is thermalized.

At 25°C, r = 0.06μ, so the probability of escape is 0.94 when y = 1μ. At 170°C, the probability is 0.96. Hence

we can conclude that at the pressure and temperature range of these experiments we are essentially concerned with homogeneous recombination.

The recombination coefficient for homogeneous recombination in air at 25°C and at pressures in the vicinity of atmospheric has been found to be approximately 10^{-6} cc/ions sec (9). Therefore the life time (τ) of ions at a concentration of about 10^8 ions/cc would be:

$$\tau = 1/k_2 \left[M^+\right]$$

$$\tau = 1/(10^{-6} \text{ cc/(ions sec)} \times 10^8 \text{ ions/cc}$$

$$\tau = 10^{-2} \text{ sec.}$$

In helium, argon, and hydrogen the electrons would interact only slightly with the surrounding medium, and hence would be quasi free (9). The mobilities of these electrons at half an atmosphere of pressure and room temperature would be about $10^3 - 10^4$ $cm^2/(V \text{ sec})$. The life time of an electron, at electric fields (1000 V/cm) where saturation currents were obtained for most of the above gases in the cells with parallel plate electrodes separated by 2.5 cm, would be approximately

$$2.5 \text{ cm}/(10^4 \text{ cm}^2/\text{V sec} \times 1000\text{V/cm}) = 2.5 \times 10^{-7} \text{sec.}$$

From the above calculations we can infer that neutralization at the electrodes should occur to the exclusion of homogeneous recombination.

In air, the electrons attach to oxygen molecules, forming negative ions. The mobility of the negative ion

is smaller than that of the quasi-free electron by a factor of about 10^2 (11). This still leaves neutralization at the electrodes as the more favourable process.

Experimental results suggest that generally in the vicinity of 0.5 atm of pressure, the temperature dependence of the coefficient for homogeneous recombination is in the region from T^{-1} to T^{-4} over the 300 to 3000°K temperature range. Gardner's (12) results of the measurements of k_2 as a function of temperature in 1 atm of oxygen gave a temperature dependence of $T^{-3.5}$ between 200 to 380°K. Kasner (13) found that at nitrogen pressures less than 10^{-2} torr, and for neon pressures in the range 15 to 40 torr, over the temperature range, 205 to 480°K the homogeneous recombination coefficient exhibited no significant temperature dependence. At an initial pressure of 3 torr, Fox and Hobson (14) reported that the recombination coefficient varied as $T^{-3/2}$ over the 1000° to 3000°K temperature range. Fisk, Mahan, and Parks (15) found a temperature dependence of $T^{-4.1}$ for neutralization of gaseous ions generated from thallium and lead halides over the pressure range of 50 to 400 torr and between 500° to 700°K. J.J. Thomson's (16) equation for homogeneous recombination Predicts a temperature dependence of $T^{-3/2}$.

Any of the above values for temperature dependence for homogeneous recombination coefficients could give an increase in the initial slope of the current-voltage curve

but would have no effect upon the saturation currents within the dose rate, pressure, and temperature range studied.

C. Space Charges at the Electrodes Should Not Affect the Saturation Currents

Space-charges, net charges of electricity in the space near the electrodes, retard the flow of current when the number of field lines from the charges in the volume of the ionized gas is equal to an apprecieable fraction of the number of field lines from the electrodes. By comparing the number of field lines from the above sources, the current density at which field distortion by space charges becomes significant can be estimated.

The charge (11) per unit area on the parallel electrodes is $\sigma = X/4\pi$; when the current density is almost equal to the saturation current the charge in the corresponding volume is

$$eNd = dj/(k^+ + k^-)X$$

where X = field strength

N = number of ion pairs/cm^3

d = distance between the electrodes

j = current density

k^+ = mobility of positive ion

k^- = mobility of negative ion.

Field distortion has to be considered when these two

quantities become similar in magnitude.

In the Quartz cell (d = 3 cm) with a pressure of 302 torr of air at 25°C, 90% saturation currents were obtained at 233 V/cm.

By equating $X/4\pi$ to $dj/(k^+ + k^-)X$ for X = 233 V/cm and using $(k^+ + k^-) = 12$ cm^2/(V sec)(11), it is found that space charges distort the field when the current density is $\geqslant 1.9 \times 10^{-8}$ amps/cm^2.

The current obtained in the Quartz cell at 90% saturation was equal to 5.2×10^{-8} amp/cm^2. Therefore, space-charges at these voltages would distort the field.

The current at which space-charges become important increases as X^2. When 1800 volts are applied across the cell, the current at which space-charges distort the field is 1.3×10^{-7} amp/cm^2. The saturation current obtained at this voltage was 5.8×10^{-8} amp/cm^2. Thus, in the current saturation region for air, space-charges should have negligible effect on the field and the current.

The saturation currents for helium and hydrogen were lower than that for air, and therefore the importance of space-charge effects for these gases would occur at lower voltages than that for air.

Most experimental results on the influence of temperature on the mobilities of ions (16) (17), indicate that , the mobility at constant density is independent of temperature. Consquently, the

effect of space-charges on the measured current should not vary with temperature.

D. Effect too Large for Ion Loss by Diffusion to the Walls

In addition to the possible loss of ions arising from recombination, there is evidence that the ions in some gas phase radiolysis systems do not all react according to homogeneous kinetics (10); loss of some ions may arise from diffusion of ions to walls of the vessel. Most gas phase radiolysis involve gases at 0.1 - 1 atm pressure in reaction vessels that have diameters of 5-13 cm. In such systems (18, 19, 20), evidence has been found that an appreciable fraction of the hydrocarbon ions is neutralized on the vessel walls. However, in the absence of an electric field, at the irradiation dose rates used in the experiments, calculations (10, 19) indicate that the positive ions could not have diffused to the walls before being neutralized. The much more mobile electron (mainly because of the smaller mass) if allowed to diffuse freely, might have been able to diffuse to the walls, but calculations indicate that even this is on the borderline of credibility (10).

At typical dose rates used in radiation chemistry, gas-phase radiation chemistry may legitimately be thought of as a sort of plasma chemistry. According to one definition, a true plasma may be distinguished from an ordinary ensemble of ions and electrons when an ionized volume contains

ion pairs at densities of the order of 10^8 to 10^{11} pairs per cm^3 (21). Another definition states that a plasma exists when the physical extent of an ionized gas is much greater than the Debye shielding length in the gas (measure of the size of the screening ion cloud surrounding a given ion) (17).

At the dose rates used in this experimental work, ion densities were in the order of 10^8 ion pairs per cm^3. The Debye shielding length (λ_D), defined by (17)

$$\lambda_D^2 = \left[\frac{4\pi e^2}{\epsilon} \sum_j \frac{n_{j\circ} Z_j^2}{KT_j}\right]^{-1}$$

where ϵ = the dielectric constant of the medium and is essentially unity for gases at about 1 atm pressure

$n_{j\circ}$ = ions per cm^3 of type j with $Z_j e$ electronic charges per ion

K = Boltzmann's constant (1.380×10^{-16} ergs/degree)

T_j = temperature in degrees Absolute

was found to be in the vicinity of 10^{-2} cm. The cylindrical cells used were 2.5 cm long with a 5-cm diameter. Therefore, under the conditions of this study, the ionized gas was a plasma.

The forces acting between neutral molecules have a very short range of action and become appreciable only when the particles approach each other to within 10^{-8} to

10^{-7} cm. By contrast, the Coulomb forces between the ions and electrons in a plasma have a very long range and are appreciable at larger distances (22). Because of the Coulombic interactions, diffusion of ions in a plasma differs somewhat from diffusion of neutral molecules, or of ions when the degree of ionization of the gas is small, and is called ambipolar. In ambipolar diffusion, the electrons with their greater mobilities tend to leave the slower ions behind, giving rise to a negative electric field at the vessel walls. This field repels other electrons and decreases their rate of diffusion to the walls, while slightly accelerating the heavy ions. As a result, the net velocities of ions and electrons tend to become equal, and the diffusion process occurs at a rate which is nearly the same as the rate of diffusion of neutral molecules (22).

A comparison of ionic life times with respect to homogeneous recombination and ambipolar diffusion shows that in the absence of an electric field, only an insignificant fraction of the ions would be lost due to diffusion to the walls. The lifetime of an ion before homogeneous neutralization under the conditions of this study would be

$$1/(k_2 [N_o]) \simeq 1/(10^{-6} \times 10^{8}) \simeq 10^{-2} \text{ sec.}$$

The distance x travelled by an ion in time t when diffusion is ambipolar is

$$x = (t D_a)^{1/2}$$

where D_a = ambipolar diffusion coefficient

$$\simeq 2 D_+ \simeq 1 \text{ (5, 11)}$$

Thus $x \doteq 10^{-1}$ cm.

Hence, the fraction of the ions that could reach the walls of the radiolysis cells used before recombining would be negligible. In the presence of an electric field, there should be no loss of ions due to ambipolar diffusion.

Klots and Anderson (23) have described a general method of calculating the relative extents of diffusional and gas-phase ion loss. They defined a dimensionless parameter, k, given by

$$k^2 = R^4 I\alpha / D+ \; D-$$

where R = effective radius of the vessel

I = rate of formation of ions

α = homogeneous bimolecular recombination coefficient

D+, D- = positive and negative diffusion coefficients.

For the present experiments with air and hydrogen at 300 torr, R = 3 cm, D_a for air $\doteq$ .16 cm^2/sec (11), D_a for hydrogen $\doteq$ .68 cm^2/sec (11), I $\doteq 10^{11}$ ions/(cm^3 sec) (see p 68), and $\doteq 10^{-6}$ cm^3/(ion sec) (see p 68), the values for k were calculated to be 3.4×10^4 for air and 4.5×10^3 for hydrogen. From these data for k, and from figure 1 of Klots and Anderson (23) it may be assumed that this corresponds to almost complete loss of ions due to homogeneous recombination to the exclusion of ion loss by diffusion for air and hydrogen. This is consistent with the previous

calculations in this thesis.

Data of Back and co-workers (24,25) and of McGowan (26) also indicate that ion loss by diffusion to the vessel walls in the present work should be negligible.

E. Photoelectric Effect Should Have No Effect on the Number of Electrons Released as the Temperature is Varied in the Present Range

Millikan and Winchester (27) investigated the effect of temperature on the total number of photo-electrons set free from a metal surface. They found that the number of electrons liberated from a metal was not affected by variations of temperature within the temperature range 50° to 343°C. The number of photo electrons, liberated from a metal is dependent upon the energy of the ultra-violet light and the work function of the metal. It is reasonable to assume that the number of Compton electrons would also be temperature independent over the range studied. For thermionic emission of electrons, temperature in the vicinity of 2000°C is required (28).

3. INTERPRETATION OF EFFECTS IN PYREX CELLS

A. General Interpretation of the Temperature Effects

The following discussion applies to the "saturation current region", in which sufficient voltage is applied across the cell to collect all of the gaseous

ions at the electrodes.

For the sake of simplicity, the interpretation of the temperature effects will be presented first. The interpretation will be substantiated in the later discussion.

At room temperature all the gaseous ions are collected on the collecting electrode, and the conductance of the Pyrex glass is negligible. The ammeter (Am in Fig IV - 1A) therefore registers the true saturation current. At temperatures greater than 50°C the Pyrex conducts appreciably, so the total current flowing in the circuit is greater than the gas phase saturation current. Furthermore, when the Pyrex becomes a conductor the walls of the Pyrex cell also act as collecting electrodes, so all the ions are not collected on the metal electrodes. If the outer surface of the cell is insulated, the total current in the circuit passes through the meter Am. However, if the outer surface of the cell is grounded, part of the current by-passes the meter (Fig IV - 1B). The fraction of the total current that by-passes the meter depends on the relative resistances of the two grounding paths. For example, when the cell is in the gamma radiation field, the ionized air surrounding the cell provides an electrical shunting path. At temperatures greater than 110°, the conductance of the Pyrex becomes so large that, when the cell is in the radiation field, the amount of current shunted through the ionized air is greater than the current due to the collection of

FIGURE IV - 1

Interpretation of Effects in Pyrex Cells

A. Current Measurements When Pyrex Cell Wall Does Not Conduct

$i_o = i_s$

i_o = total current in circuit

i_s = saturation current

B. Current Measurements When Pyrex Cell Wall Conducts

$i_o = i_1 + i_2 > i_s$

i_1, and i_2 each contain components due to collection of gaseous ions in the cell and to conductance of the glass.

A

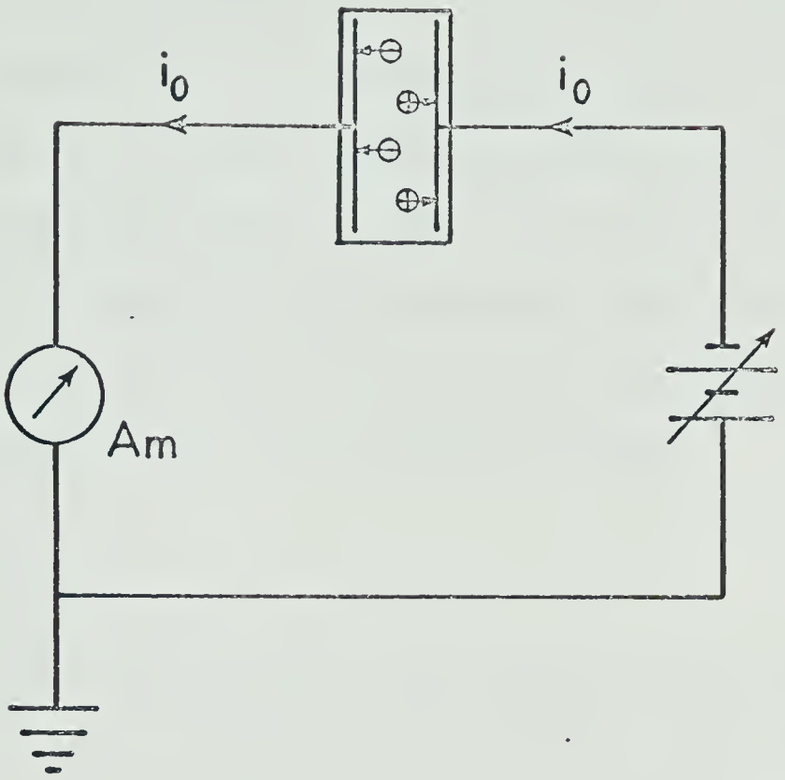

B

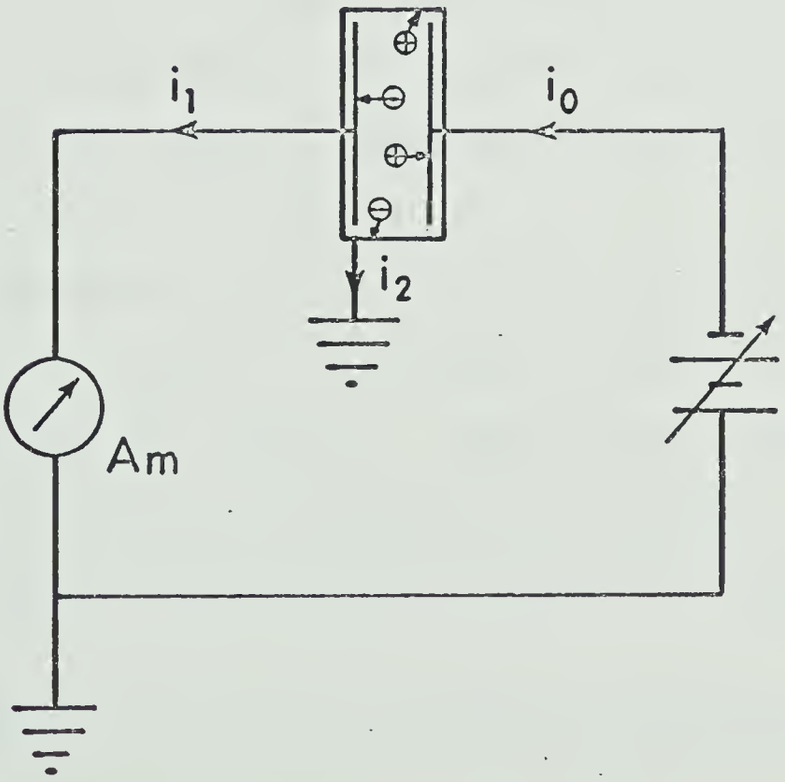

gaseous ions in the cell. In the absence of a radiation field, the outer surface of a clean Pyrex cell is not grounded, so the total current passes through the meter Am. When the cell is lowered into the radiation field the outer surface becomes grounded. Thus, at temperatures greater than 110°, the unsettling observation was made that the current through the meter Am actually decreased when the cell was lowered into the radiation field.

B. Pyrex Plug

The conductance of the solid Pyrex plug (Fig II - 2B) was appreciable at temperatures greater than 50°. The apparent conductance of the unwrapped plug, as indicated by the current passing through the ammeter, was greater in the absence than in the presence of the radiation field (Table III - 3). This is because the ionized air in the radiation field partially grounded the plug and diverted some of the current from the ammeter, similar to the situation represented in Fig. IV - 1B.

Insulation of the plug from the ionized air, by wrapping the plug with teflon tape, forced all the current to pass through the ammeter. Under these conditions the apparent conductance corresponded to the true conductance, and was larger in the presence than in the absence of the radiation.

When no external voltage was applied to the plug,

there was a current in the circuit. The current increased with increasing temperature and was larger in the presence than in the absence of radiation (Tables III - 3 and 4, pp 51-2). This current was also generated at the Pyrex-tungsten junctions in the gas cells, but it was sufficiently small that it did not interfere with the current measurements in the gases.

C. Parallel-Plate Cell

The saturation currents measured in air and helium were independent of temperature in the range from -196° to +50°C. At temperatures above 50°, the saturation currents for air, argon, helium, and hydrogen appeared to decrease. This was caused by the Pyrex cell wall becoming a conductor at the higher temperatures. Thus, in the absence of a radiation field, a high "background" current was recorded. In the presence of a radiation field, part of this background current is shorted to ground through the ionized air, so the current passing through the ammeter was reduced. The saturation current i_s passing through the gas in the cell was initially assumed to be equal to

$$i_s = i_r + i_b$$

where i_r was the current passing through the ammeter when the cell was in the radiation field and i_b was the background current when the cell was out of the radiation

field. However, as indicated by the experiments with the solid Pyrex plug, the actual background current was smaller in the presence than in the absence of the radiation field, so equation $i_s = i_r + i_b$ gives values of i_s that are too small at temperatures greater than 50°.

The following experiments support the above experiments.

When the cell was wrapped with teflon tape it was isolated from the ionized air and practically temperature independent values of i_s were obtained.

Painting the outer surface of the cell around the collecting electrode with aquadag and grounding it with a copper wire (Fig. IV - 1A) increased the temperature dependence of the saturation currents (pp 42-6). Since now the relative resistance of the grounded path was much lower than that of the ionized air, the background currents (i_b) became negligible at all temperatures, and the measured saturation currents (i_s) were greatly reduced since the gaseous ions could be more easily conducted to ground. Painting a larger surface area enhanced the above observations since a larger portion of the outer surface was more effectively grounded. It was also observed that the positive saturation currents decreased to a greater extent than did the negative saturation currents. This can be explained by the fact that Pyrex is a better conductor of positive ions than of negative ions (30).

Different surface areas of the gas were put in contact with the cell walls by varying the ratio of the diameter (d) of the electrodes to the distance (l) between the electrodes. The saturation currents decreased as the ratio of (d) to (l) decreased (Fig III-9) and confirmed the theory that the efficiency for ion collection of a parallel-plate radiolysis cell increases with larger electrodes and with a smaller distance between them. The temperature effect decreased with increasing (d/l), as expected.

As mentioned in Section A, it was noticed that the effect of temperature on the saturation currents decreased as the mass of the ions increased. This is in keeping with the kinetic theory of gases which states that the mobility (u) of an ion is roughly inversely proportional to the square root of the mass of the ion or

$$u = e\lambda_i(\pi/\ 8MkT)^{\frac{1}{2}}$$

Where e = charge of the ion

λ_i = the ionic mean free path

M = mass of the ion

k = Boltzmann's constant

T = absolute temperature

Similarly a progressive shift of the ion collection sigmoid curve towards higher voltages was obtained in going from hydrogen to helium to air and to argon. This could also be attributed as being due to the differences in

the mass of the ions.

Saturation current measurements indicated that the decrease of the saturation currents with increasing temperature were greater in the cell with aluminium electrodes than in the cell with platinium and aquadag electrodes. This could not be explained as being due to differences in dose rate caused by differences in the electron density of the electrodes since platinium and aquadag have dissimilar electron densities and still gave the same decrease in the net currents. The cause of the difference is not known.

That conditioning the cell reduced the percent decrease of the hydrogen saturation currents but did not affect the helium saturation currents could be explained by the fact that hydrogen is more reactive than helium and could temporarily change the composition of the Pyrex cell wall.

The many obstacles encountered in the collection of ions in air and in argon in the Pyrex cell with a platinium collecting electrode surrounded by a guard ring (Fig II-1B) made it difficult to interpret the results obtained in this cell. However, in several of the current measurements it was observed that the decrease in the positive saturation currents were less in the cell with guard rings than in the cell without guard rings. This is further evidence that the decrease in the current was partly due to the collection of ions by the Pyrex cell wall.

D. Spherical Cell

A Pyrex spherical cell with painted aquadag electrodes gave larger saturation currents as the temperature of the gas and cell was increased. The increase in the positive saturation currents was greater than that of the negative saturation current (Fig III-10,11). It was surmised that when the walls of the Pyrex spherical cell conduct, the field at the cell is greater than the field of the surrounding ionized air, and ions from outside the cell are collected at the walls. Since Pyrex is a better conductor of positive charges than of negative charges, when the outer spherical electrode is positive, a large number of the negative charges are neutralized by the positive charges before they are conducted to the electrometer. Therefore only a slight increase in the negative saturation current is observed. When the outside electrode of the spherical cell is negative, the positive charges from the surrounding ionized air are readily conducted by the Pyrex, and a significant increase in the positive saturation current is measured. When the spherical cell was wrapped with teflon tape, there was only a slight increase in the saturation current (Fig III-12). The teflon tape prevented the charges from the surrounding ionized air from being collected on the cell.

4. TEMPERATURE INDEPENDENT CURRENTS WERE OBTAINED IN QUARTZ CELL

After the conductivity of a Quartz plug at 110° and 170°C was found to be smaller than the conductivity of the of the Pyrex plug by factors of 10 and 10,000, respectively, a Quartz cell with stainless steel electrodes was made. Current measurements taken in this cell gave only a 2% decrease in the saturation currents at 170° from the 25° value for air, and a 0.5% decrease for hydrogen. I_b was very small, and consequently i_s was equal to i_r. Hence these results support the thesis that the conducting Pyrex acts partly as an electrode at the elevated temperatures and is responsible for the complications in the current measurements at these temperatures.

5. DOSE RATE STUDIES

The dose rate studies indicated that space charges and better conductance of positive charges were also determining factors in the temperature dependent currents. Since the decreases in the saturation currents from the 25° value were somewhat more pronounced at the lower dose rates, it could be possible that at the higher dose rates the space charges along the cell wall tend to prevent ions from collecting on the wall. There is less interference with ion collection and consequently a smaller decrease in the saturation currents.

The greater decreases in the positive current than in the negative current for hydrogen in the Pyrex cell can

be explained by the facts that cations migrate through glass more readily than do anions and that the resistivity of of glasses that conduct by an electronic mechanism is greater than of glasses that conduct by a cationic mechanism (30). In hydrogen, the charges would be mostly cations and electrons, and therefore both of the above factors would contribute to the results as obtained in Fig III-14. The effects for hydrogen in the Quartz cell are greatly reduced, since as already mentioned previously, the conductivity of Quartz is much smaller than the conductivity of Pyrex at elevated temperatures. This gives further proof that Quartz cells are more desireable than Pyrex cells for the temperature study of ion collection.

6. TEMPERATURE INDEPENDENT CURRENTS IN EXTERNALLY INSULATED SPHERICAL STAINLESS STEEL CELLS

The absence of a temperature effect on the saturation currents obtained in an externally insulated spherical stainless steel cell (Fig III-13) gave further evidence that the grounding of the conducting Pyrex cell wall by the ionized air was responsible for the decrease in the saturation currents at the elevated temperatures.

REFERENCES

1. G. R. Freeman, "Radiation Chemistry Notes", University of Alberta.
2. J. Spinks and R. Woods, "An Introduction to Radiation Chemistry", John Wiley & Sons, New York, 1964.
3. W. J. Holtslander, Ph. D. Thesis, University of Alberta, 1966.
4. F. T. Jones and T. J. Sworski, J. Phys. Chem. 70, 1546, 1966.
5. G. R. Freeman, Private Communication.
6. R. K. McClung, Phil. Mag. 7, 81, 1904.
7. J. A. Crowther, Proc. Roy. Soc. 82, 351, 1909.
8. A. H. Compton, R. D. Bennett, J. C. Stearns, Phys. Rev. 39, 873, 1932.
9. G. R. Freeman, The Chemistry of the Carbonyl Group, Part 2, J.Zabicky (Ed.), in the press.
10. G. R. Freeman, Radiation Research Reviews, 1, 1-74, 1968.
11. A von Engel, "Ionized Gases", 2nd ed., Clarendon Press, Oxford, 1965.
12. M. E. Gardner, Phys. Rev. 53, 75, 1938.
13. W. H. Kasner, The Phys. Rev. 164, 194, 1967.
14. J. N. Fox and R. M. Hobson, Physical Review Letters 17, 161, 1966.
15. G. A. Fisk, B. H. Mahan, E. K. Parks, J. Chem. Phys. 47, 2649, 1967.

16. J. J. Thompson and G. P. Thompson, "Conduction of Electricity Through Gases", 3rd ed., Cambridge University Press, 1928.

17. E. W. McDaniel, "Collision Phenomena in Ionized Gases", John Wiley & Sons, New York, 1964.

18. R. A. Back, T. W. Woodward and K. A. McLauchlan, Can. J. Chem. 40, 1380, 1962.

19. T. W. Woodward and R. A. Back, Can. J. Chem. 41, 1463, 1963.

20. L. I. Bone, L. W. Sieck and J. H. Futrell, J. Chem. Phys., 44, 3667, 1966.

21. R. L. Ramey, "Physical Electronics", Wadsworth Publishing Co., Belmont, 1961.

22. L. A. Arzimovich, "Elementary Plasma Physics", Blaisdell Publishing Co., Toronto, 1965.

23. C. E. Klots and V. E. Anderson, J. Phys. Chem. 71, 265, 1967.

24. C. J. Wood, R. A. Back, D. H. Dawes, Can. J. Chem. 45, 3071, 1967.

25. D. A. Armstrong, R. A. Back, Can. J. Chem. 45, 3079, 1967.

26. S. McGowan, Can. J. of Phys. 45, 429, 1967.

27. R. A. Millikan and G. Winchester, Phil. Mag. 14, 188, 1907.

28. H. Semat and R. Kotz, "Physics", Rinehart & Co. Inc., 1958.

29. O. W. Richardson, "Emission of Electricity from Hot Bodies", Longmans, Green & Co., 1916.

30. O. V. Mazurin, "Electrical Properties and Structure of Glass", Consultants Bureau, New York, 1965.